

## 2. THE PHYSICS OF DIFFRACTION GRATINGS

---

PREVIOUS CHAPTER  
NEXT CHAPTER

Copyright 2002, Thermo RGL,  
All Rights Reserved

### TABLE OF CONTENTS

- 2.1. THE GRATING EQUATION
- 2.2. DIFFRACTION ORDERS
  - 2.2.1. *Existence of Diffraction Orders*
  - 2.2.2. *Overlapping of Diffracted Spectra*
- 2.3. DISPERSION
  - 2.3.1. *Angular dispersion*
  - 2.3.2. *Linear dispersion*
- 2.4. RESOLVING POWER, SPECTRAL RESOLUTION, AND BANDPASS
  - 2.4.1. *Resolving power*
  - 2.4.2. *Spectral resolution*
  - 2.4.3. *Bandpass*
  - 2.4.4. *Resolving power vs. resolution*
- 2.5. FOCAL LENGTH AND  $f$ /NUMBER
- 2.6. ANAMORPHIC MAGNIFICATION
- 2.7. FREE SPECTRAL RANGE
- 2.8. ENERGY DISTRIBUTION (GRATING EFFICIENCY)
- 2.9. SCATTERED AND STRAY LIGHT
  - 2.9.1. *Scattered light*
  - 2.9.2. *Instrumental stray light*
- 2.10. SIGNAL-TO-NOISE RATIO (SNR)

## 2.1. THE GRATING EQUATION [\[top\]](#)

When monochromatic light is incident on a grating surface, it is diffracted into discrete directions. We can picture each grating groove as being a very small, slit-shaped source of diffracted light. The light diffracted by each groove combines to form a diffracted wavefront. The usefulness of a grating depends on the fact that there exists a unique set of discrete angles along which, for a given spacing  $d$  between grooves, the diffracted light from each facet is in phase with the light diffracted from any other facet, so they combine constructively.

Diffraction by a grating can be visualized from the geometry in Figure 2-1, which shows a light ray of wavelength  $\lambda$  incident at an angle  $\alpha$  and diffracted by a grating (of *groove spacing*  $d$ , also called the *pitch*) along angles  $\beta_m$ . These angles are measured from the grating normal, which is the dashed line perpendicular to the grating surface at its center. The sign convention for these angles depends on whether the light is diffracted on the same side or the opposite side of the grating as the incident light. In diagram (a), which shows a *reflection grating*, the angles  $\alpha > 0$  and  $\beta_1 > 0$  (since they are measured counter-clockwise from the grating normal) while the angles  $\beta_0 < 0$  and  $\beta_{-1} < 0$  (since they are measured clockwise from the grating normal). Diagram (b) shows the case for a *transmission grating*.

By convention, angles of incidence and diffraction are measured *from* the grating normal *to* the beam. This is shown by arrows in the diagrams. In both diagrams, the sign convention for angles is shown by the plus and minus symbols located on either side of the grating normal. For either reflection or transmission gratings, the algebraic signs of two angles differ if they are measured from opposite sides of the grating normal. Other sign conventions

---

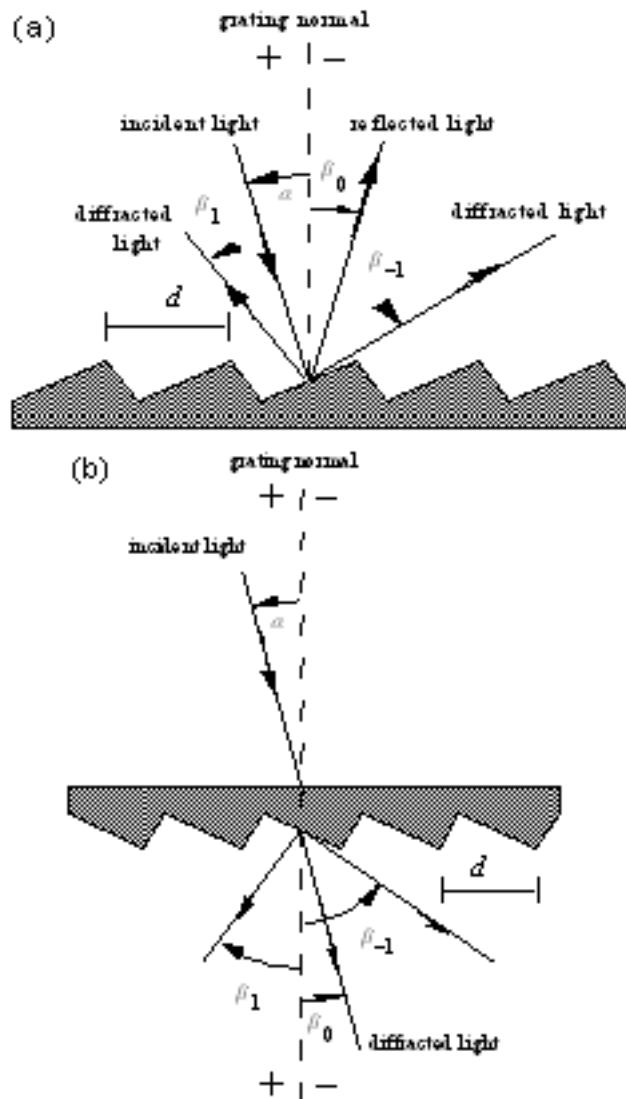


*Figure 2-1. Diffraction by a plane grating.* A beam of monochromatic light of wavelength  $\lambda$  is incident on a grating and diffracted along several discrete paths. The triangular grooves come out of the page; the rays lie in the plane of the page. The sign convention for the angles  $\alpha$  and  $\beta$  is shown by the + and - signs on either side of the grating normal. (a) A *reflection grating*: the incident and diffracted rays lie on the same side of the grating. (b) A *transmission grating*: the incident and diffracted rays lie on opposite sides of the grating.

exist, so care must be taken in calculations to ensure that results are self-consistent. Another illustration of grating diffraction, using wavefronts (surfaces of constant phase), is shown in Figure 2-2. The geometrical path difference between light from adjacent grooves is seen to be  $d \sin\alpha + d \sin\beta$ . [Since  $\beta < 0$ , the latter term is actually negative.] The principle of interference

dictates that only when this difference equals the wavelength  $\lambda$  of the light, or some integral multiple thereof, will the light from adjacent grooves be in phase (leading to constructive interference). At all other angles  $\beta$ , there will be some measure of destructive interference between the wavelets originating from the groove facets.

These relationships are expressed by the *grating equation*

$$m\lambda = d (\sin\alpha + \sin\beta), \quad (2-1)$$

which governs the angles of diffraction from a grating of groove spacing  $d$ . Here  $m$  is the *diffraction order* (or *spectral order*), which is an integer. For a particular wavelength  $\lambda$ , all values of  $m$  for which  $|m\lambda/d| < 2$  correspond to physically realizable diffraction orders.

It is sometimes convenient to write the grating equation as

$$Gm\lambda = \sin\alpha + \sin\beta, \quad (2-1')$$

where  $G = 1/d$  is the *groove frequency* or *groove density*, more commonly called "grooves per millimeter".

Eq. (2-1) and its equivalent Eq. (2-1') are the common forms of the grating equation, but their validity is restricted to cases in which the incident and diffracted rays are perpendicular to the grooves (at the center of the grating). The vast majority of grating systems fall within this category, which is called *classical* (or *in-plane*) *diffraction*. If the incident light beam is not perpendicular to the grooves, though, the grating equation must be modified:

$$Gm\lambda = \cos\epsilon (\sin\alpha + \sin\beta), \quad (2-1'')$$

Here  $\epsilon$  is the angle between the incident light path and the plane perpendicular to the grooves at the grating center (the plane of the page in Figure 2-2). If the incident light lies in this plane,  $\epsilon = 0$  and Eq. (2-1'') reduces to the more familiar Eq. (2-1'). In geometries for which  $\epsilon \neq 0$ , the diffracted spectra lie on a cone rather than in a plane, so such cases are termed *conical diffraction*.

For a grating of groove spacing  $d$ , there is a purely mathematical relationship

between the wavelength and the angles of incidence and diffraction. In a given spectral order  $m$ , the different wavelengths of polychromatic wavefronts incident at angle  $\alpha$  are separated in angle:

$$\beta(\lambda) = \arcsin(m\lambda/d - \sin\alpha). \quad (2-2)$$

When  $m = 0$ , the grating acts as a mirror, and the wavelengths are not separated ( $\beta = -\alpha$  for all  $\lambda$ ); this is called *specular reflection* or simply the *zero order*.

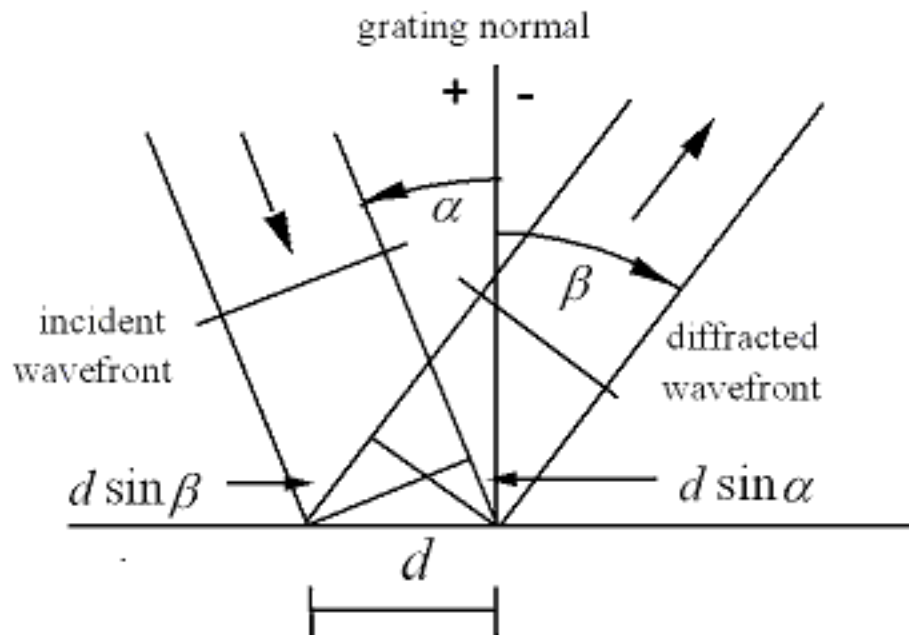


Figure 2-2. Geometry of diffraction, for planar wavefronts. The terms in the path difference,  $d \sin\alpha$  and  $d \sin\beta$ , are shown.

A special but common case is that in which the light is diffracted back toward the direction from which it came (i.e.,  $\alpha = \beta$ ); this is called the *Littrow configuration*, for which the grating equation becomes

$$m\lambda = 2d \sin\alpha, \quad \text{in Littrow.} \quad (2-3)$$

In many applications (such as constant-deviation monochromators), the wavelength  $\lambda$  is changed by rotating the grating about the axis coincident with

its central ruling, with the directions of incident and diffracted light remaining unchanged. The *deviation angle*  $2K$  between the incidence and diffraction directions (also called the *angular deviation*) is

$$2K = \alpha - \beta = \text{constant} \quad (2-4)$$

while the scan angle  $\phi$ , which is measured from the grating normal to the bisector of the beams, is

$$2\phi = \alpha + \beta. \quad (2-5)$$

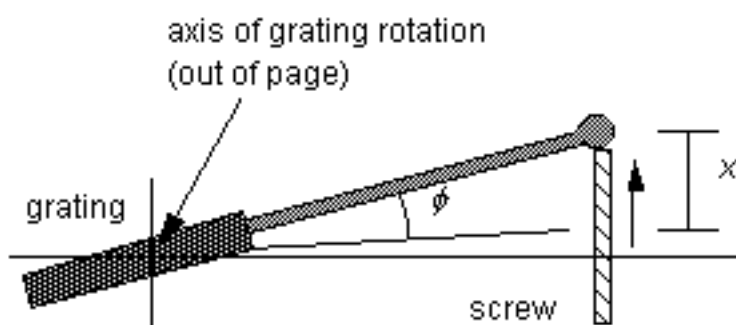


*Figure 2-3. A sine bar mechanism for wavelength scanning. As the screw is extended linearly by the distance  $x$  shown, the grating rotates through an angle  $\phi$  in such a way that  $\sin\phi$  is proportional to  $x$ .*

Note that  $\phi$  changes with  $\lambda$  (as do  $\alpha$  and  $\beta$ ). In this case, the grating equation can be expressed in terms of  $\phi$  and the *half deviation angle*  $K$  as

$$m\lambda = 2d \cos K \sin\phi. \quad (2-6)$$

This version of the grating equation is useful for monochromator mounts (see [Chapter 7](#)). Eq. (2-6) shows that the wavelength diffracted by a grating in a monochromator mount is directly proportional to the sine of the angle  $\phi$  through which the grating rotates, which is the basis for monochromator drives in which a sine bar rotates the grating to scan wavelengths (see Figure 2-3).

## 2.2. DIFFRACTION ORDERS [\[top\]](#)

### 2.2.1. Existence of Diffraction Orders.

For a particular set of values of the groove spacing  $d$  and the angles  $\alpha$  and  $\beta$ , the grating equation (2-1) is satisfied by more than one wavelength. In fact, subject to restrictions discussed below, there may be several discrete wavelengths which, when multiplied by successive integers  $m$ , satisfy the condition for constructive interference. The physical significance of this is that the constructive reinforcement of wavelets diffracted by successive grooves merely requires that each ray be retarded (or advanced) in phase with every other; this phase difference must therefore correspond to a real distance (path difference) which equals an integral multiple of the wavelength. This happens, for example, when the path difference is one wavelength, in which case we speak of the positive first diffraction order ( $m = 1$ ) or the negative first diffraction order ( $m = -1$ ), depending on whether the rays are advanced or retarded as we move from groove to groove. Similarly, the second order ( $m = 2$ ) and negative second order ( $m = -2$ ) are those for which the path difference between rays diffracted from adjacent grooves equals two wavelengths.

The grating equation reveals that only those spectral orders for which  $|m\lambda/d| < 2$  can exist; otherwise,  $|\sin\alpha + \sin\beta| > 2$ , which is physically meaningless. This restriction prevents light of wavelength  $\lambda$  from being diffracted in more than a finite number of orders. Specular reflection ( $m = 0$ ) is always possible; that is, the *zero order* always exists (it simply requires  $\beta = -\alpha$ ). In most cases, the grating equation allows light of wavelength  $\lambda$  to be diffracted into both negative and positive orders as well. Explicitly, spectra of all orders  $m$  exist for which

$$-2d < m\lambda < 2d, \quad m \text{ an integer.} \quad (2-7)$$

For  $1/d \ll 1$ , a large number of diffracted orders will exist.

As seen from Eq. (2-1), the distinction between negative and positive spectral orders is that

$$\begin{aligned}
 \beta &> -\alpha && \text{for positive orders } (m > 0), \\
 \beta &< -\alpha && \text{for negative orders } (m < 0), \\
 \beta &= -\alpha && \text{for specular reflection } (m = 0),
 \end{aligned}
 \tag{2-8}$$

This sign convention for  $m$  requires that  $m > 0$  if the diffracted ray lies to the left (the counter-clockwise side) of the zero order ( $m = 0$ ), and  $m < 0$  if the diffracted ray lies to the right (the clockwise side) of the zero order. This convention is shown graphically in Figure 2-4.

### 2.2.2. Overlapping of Diffracted Spectra.

The most troublesome aspect of multiple order behavior is that successive spectra overlap, as shown in Figure 2-5. It is evident from the grating equation that, for any grating instrument configuration, the light of wavelength  $\lambda$  diffracted in the  $m = 1$  order will coincide with the light of wavelength  $\lambda/2$  diffracted in the  $m = 2$  order, *etc.*, for all  $m$  satisfying inequality (2-7). In this example, the red light (600 nm) in the first spectral order will overlap the ultraviolet light (300 nm) in the second order. A detector sensitive at both wavelengths would see both simultaneously. This superposition of wavelengths, which would lead to ambiguous spectroscopic data, is inherent in the grating equation itself and must be prevented by suitable filtering (called *order sorting*), since the detector cannot generally distinguish between light of different wavelengths incident on it (within its range of sensitivity). [See also [Section 2.7](#) below.]

## 2.3. DISPERSION [\[top\]](#)

The primary purpose of a diffraction grating is to disperse light spatially by wavelength. A beam of white light incident on a grating will be separated into its component colors upon diffraction from the grating, with each color diffracted along a different direction. *Dispersion* is a measure of the separation (either angular or spatial) between diffracted light of different wavelengths. Angular dispersion expresses the spectral range per unit angle, and linear resolution expresses the spectral range per unit length.



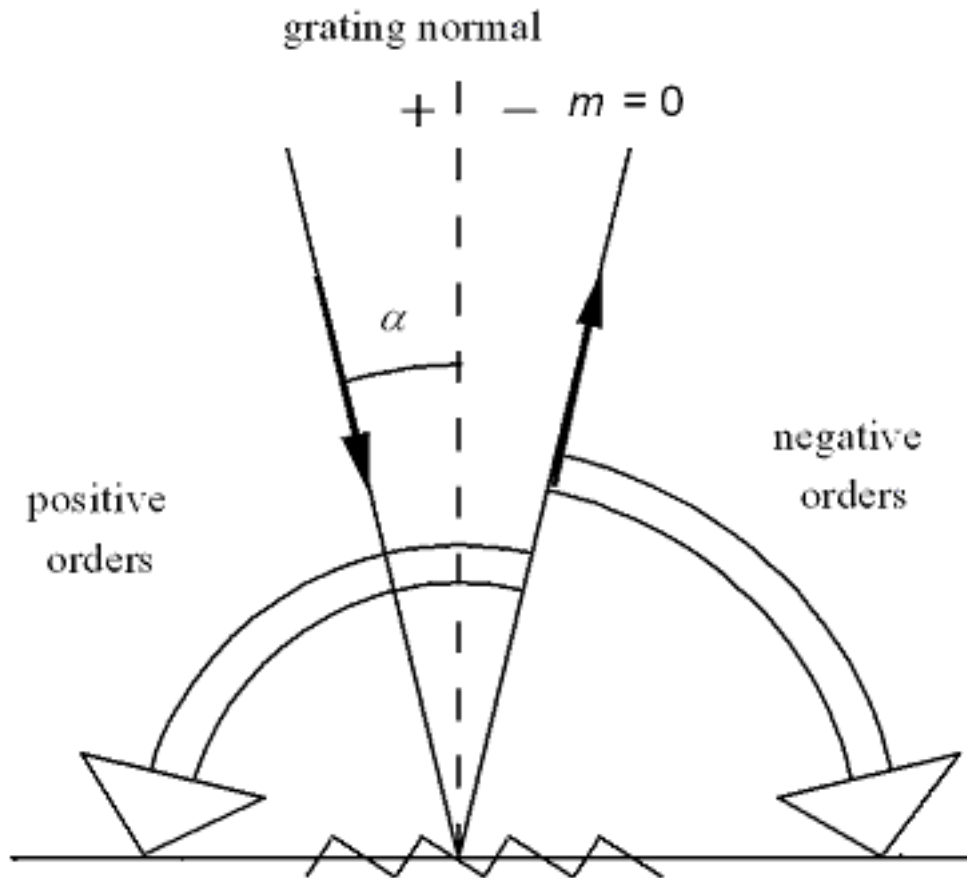


*Figure 2-4. Sign convention for the spectral order  $m$ . In this example  $\alpha$  is positive.*

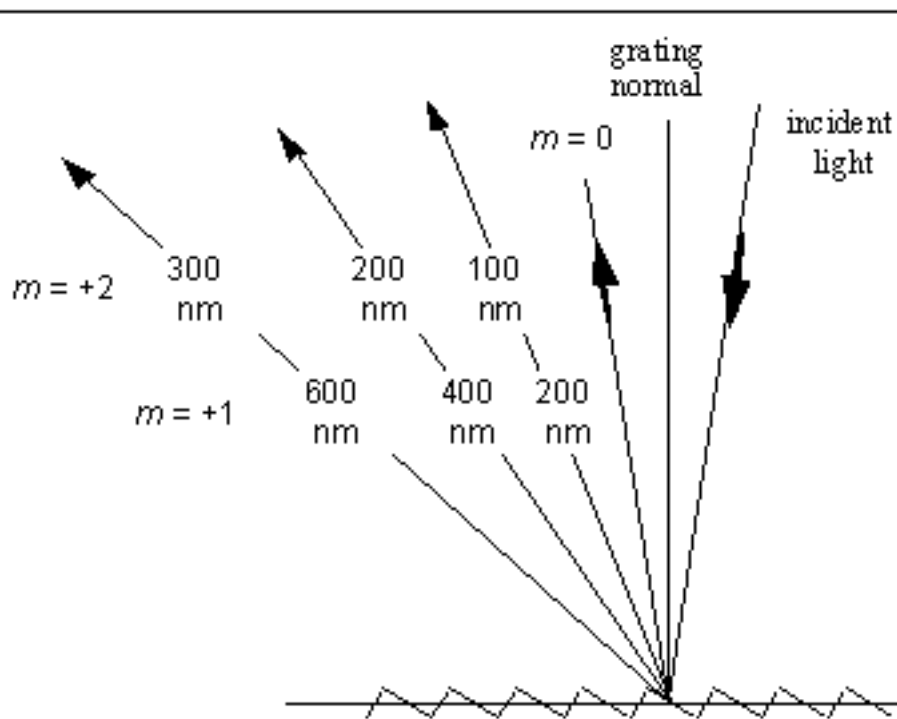


Figure 2-5. Overlapping of spectral orders. The light for wavelengths 100, 200 and 300 nm in the second order is diffracted in the same direction as the light for wavelengths 200, 400 and 600 nm in the first order. In this diagram, the light is incident from the right, so  $\alpha < 0$ .

### 2.3.1. Angular dispersion

The angular spread  $d\beta$  of a spectrum of order  $m$  between the wavelength  $\lambda$  and  $\lambda + d\lambda$  can be obtained by differentiating the grating equation, assuming the incidence angle  $\alpha$  to be constant. The change  $D$  in diffraction angle per unit wavelength is therefore

$$D = \frac{\partial\beta}{\partial\lambda} = \frac{m}{d \cos\beta} = \frac{m}{d} \sec\beta = Gm \sec\beta \quad (2-9)$$

where  $\beta$  is given by Eq. (2-2). The ratio  $D = d\beta / d\lambda$  is called the *angular dispersion*. As the groove frequency  $G = 1/d$  increases, the angular dispersion increases (meaning that the angular separation between wavelengths increases

for a given order  $m$ ).

In Eq. (2-9), it is important to realize that the quantity  $m/d$  is not a ratio which may be chosen independently of other parameters; substitution of the grating equation into Eq. (2-9) yields the following general equation for the angular dispersion:

$$D = \frac{\partial \beta}{\partial \lambda} = \frac{\sin \alpha + \sin \beta}{\lambda \cos \beta} \quad (2-10)$$

For a given wavelength, this shows that the angular dispersion may be considered to be solely a function of the angles of incidence and diffraction. This becomes even more clear when we consider the Littrow configuration ( $\alpha = \beta$ ), in which case Eq. (2-10) reduces to

$$D = \frac{\partial \beta}{\partial \lambda} = \frac{2}{\lambda} \tan \beta, \quad \text{in Littrow.} \quad (2-11)$$

When  $|\beta|$  increases from  $10^\circ$  to  $63^\circ$  in Littrow use, the angular dispersion increases by a factor of ten, regardless of the spectral order or wavelength under consideration. Once  $\beta$  has been determined, the choice must be made whether a fine-pitch grating (small  $d$ ) should be used in a low order, or a coarse-pitch grating (large  $d$ ) such as an echelle grating should be used in a high order. [The fine-pitched grating, though, will provide a larger free spectral range; see [Section 2.7](#) below.]

### 2.3.2. Linear dispersion

For a given diffracted wavelength  $\lambda$  in order  $m$  (which corresponds to an angle of diffraction  $\beta$ ), the *linear dispersion* of a grating system is the product of the angular dispersion  $D$  and the effective focal length  $r'$  ( $\beta$ ) of the system:

$$r'D = r' \frac{\partial \beta}{\partial \lambda} = \frac{mr'}{d \cos \beta} = \frac{mr'}{d} \sec \beta = Gmr' \sec \beta. \quad (2-12)$$

The quantity  $r' d\beta = dl$  is the change in position along the spectrum (a real distance, rather than a wavelength). We have written  $r'(\beta)$  for the focal length to show explicitly that it may depend on the diffraction angle  $\beta$  (which, in turn, depends on  $\lambda$ ).

The *reciprocal linear dispersion*, also called the *plate factor*  $P$ , is more often considered; it is simply the reciprocal of  $r' D$ , usually measured in nm/mm:

$$P = \frac{d \cos \beta}{m r'}. \quad (2-12')$$

$P$  is a measure of the change in wavelength (in nm) corresponding to a change in location along the spectrum (in mm). It should be noted that the terminology *plate factor* is used by some authors to represent the quantity  $1/\sin\Phi$ , where  $\Phi$  is the angle the spectrum makes with the line perpendicular to the diffracted rays (see Figure 2-6); in order to avoid confusion, we call the quantity  $1/\sin\Phi$  the *obliquity factor*. When the image plane for a particular wavelength is not perpendicular to the diffracted rays (i.e., when  $\Phi \neq 90^\circ$ ),  $P$  must be multiplied by the obliquity factor to obtain the correct reciprocal linear dispersion in the image plane.

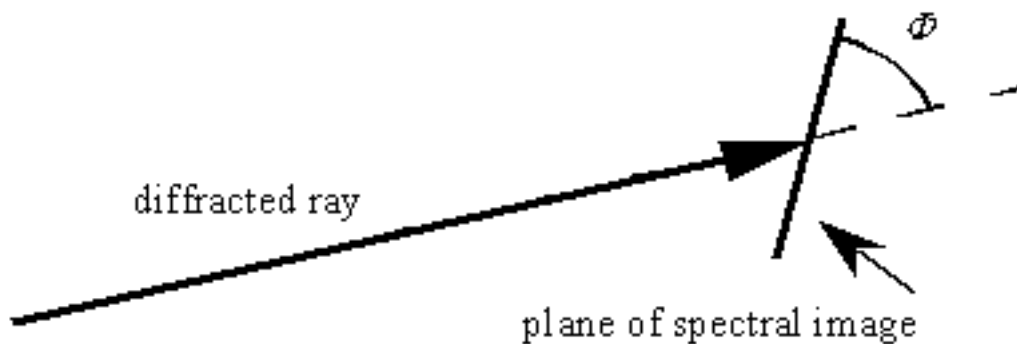


*Figure 2-6. The obliquity angle  $\Phi$ . The spectral image recorded need not lie in the plane perpendicular to the diffracted ray (i.e.,  $\Phi \neq 90^\circ$ ).*

---

## 2.4. RESOLVING POWER, SPECTRAL RESOLUTION, AND BANDPASS [\[top\]](#)

### 2.4.1. Resolving power

The resolving power  $R$  of a grating is a measure of its ability to separate adjacent spectral lines of average wavelength  $\lambda$ . It is usually expressed as the dimensionless quantity

$$R = \frac{\lambda}{\Delta\lambda}. \quad (2-13)$$

Here  $\Delta\lambda$  is the *limit of resolution*, the difference in wavelength between two lines of equal intensity that can be distinguished (that is, the peaks of two wavelengths  $\lambda_1$  and  $\lambda_2$  for which the separation  $|\lambda_1 - \lambda_2| < \Delta\lambda$  will be ambiguous). The theoretical resolving power of a planar diffraction grating is given in elementary optics textbooks as

$$R = mN. \quad (2-14)$$

where  $m$  is the diffraction order and  $N$  is the total number of grooves illuminated on the surface of the grating. For negative orders ( $m < 0$ ), the absolute value of  $R$  is considered.

A more meaningful expression for  $R$  is derived below. The grating equation can be used to replace  $m$  in Eq. (2-14):

$$R = \frac{Nd (\sin \alpha + \sin \beta)}{\lambda}. \quad (2-15)$$

If the groove spacing  $d$  is uniform over the surface of the grating, and if the grating substrate is planar, the quantity  $Nd$  is simply the ruled width  $W$  of the grating, so

$$R = \frac{W(\sin \alpha + \sin \beta)}{\lambda} \quad (2-16)$$

As expressed by Eq. (2-16),  $R$  is not dependent explicitly on the spectral order or the number of grooves; these parameters are contained within the ruled width and the angles of incidence and diffraction. Since

$$|\sin \alpha + \sin \beta| < 2 \quad (2-17)$$

the maximum attainable resolving power is

$$R_{\text{MAX}} = \frac{2W}{\lambda} \quad (2-18)$$

regardless of the order  $m$  or number of grooves  $N$ . This maximum condition corresponds to the grazing Littrow configuration, i.e.,  $\alpha \approx \beta$  (Littrow),  $|\alpha| \approx 90^\circ$  (grazing).

It is useful to consider the resolving power as being determined by the maximum phase retardation of the extreme rays diffracted from the grating. Measuring the difference in optical path lengths between the rays diffracted from opposite sides of the grating provides the maximum phase retardation; dividing this quantity by the wavelength  $\lambda$  of the diffracted light gives the resolving power  $R$ .

The degree to which the theoretical resolving power is attained depends not only on the angles  $\alpha$  and  $\beta$ , but also on the optical quality of the grating surface, the uniformity of the groove spacing, the quality of the associated optics, and the width of the slits and/or detector elements. Any departure of the diffracted wavefront greater than  $\lambda/10$  from a plane (for a plane grating) or from a sphere (for a spherical grating) will result in a loss of resolving power due to aberrations at the image plane. The grating groove spacing must be kept constant to within about 1% of the wavelength at which theoretical performance is desired. Experimental details, such as slit width, air currents, and vibrations can seriously interfere with obtaining optimal results.

The practical resolving power is limited by the spectral half-width of the

lines emitted by the source. This explains why systems with resolving powers greater than 500,000 are usually required only in the study of spectral line shapes, Zeeman effects, and line shifts, and are not needed for separating individual spectral lines.

A convenient test of resolving power is to examine the isotopic structure of the mercury emission line at 546.1 nm. Another test for resolving power is to examine the line profile generated in a spectrograph or scanning spectrometer when a single mode laser is used as the light source. Line width at half intensity (or other fractions as well) can be used as the criterion. Unfortunately, resolving power measurements are the convoluted result of all optical elements in the system, including the locations and dimensions of the entrance and exit slits and the auxiliary lenses and mirrors, as well as the quality of these optics. Their effects are necessarily superimposed on those of the grating.

### 2.4.2. Spectral resolution

While resolving power can be considered a characteristic of the grating and the angles at which it is used, the ability to resolve two wavelengths  $\lambda_1$  and  $\lambda_2 = \lambda_1 + \Delta\lambda$  generally depends not only on the grating but on the dimensions and locations of the entrance and exit slits (or detector elements), the aberrations in the images, and the magnification of the images. The minimum wavelength difference  $\Delta\lambda$  (also called the *limit of resolution*, or simply *resolution*) between two wavelengths that can be resolved unambiguously can be determined by convoluting the image of the entrance aperture (at the image plane) with the exit aperture (or detector element). This measure of the ability of a grating system to resolve nearby wavelengths is arguably more relevant than is resolving power, since it takes into account the image effects of the system. While resolving power is a dimensionless quantity, resolution has spectral units (usually nanometers).

### 2.4.3. Bandpass

The *bandpass*  $B$  of a spectroscopic system is the wavelength interval of the light that passes through the exit slit (or falls onto a detector element). It is

often defined as the difference in wavelengths between the points of half-maximum intensity on either side of an intensity maximum. An estimate for bandpass is the product of the exit slit width  $w'$  and the reciprocal linear dispersion  $P$ :

$$B \approx w' P. \quad (2-19)$$

An instrument with smaller bandpass can resolve wavelengths that are closer together than an instrument with a larger bandpass. Bandpass can be reduced by decreasing the width of the exit slit (to a certain limit; see Chapter 8), but usually at the expense of decreasing light intensity as well.

Bandpass is sometimes called *spectral bandwidth*, though some authors assign distinct meanings to these terms.

#### 2.4.4. Resolving power vs. resolution

In the literature, the terms *resolving power* and *resolution* are sometimes interchanged. While the word *power* has a very specific meaning (energy per unit time), the phrase *resolving power* does not involve *power* in this way; as suggested by Hutley, though, we may think of resolving power as 'ability to resolve'.

The comments above regarding resolving power and resolution pertain to planar classical gratings used in collimated light (plane waves). The situation is complicated for gratings on concave substrates or with groove patterns consisting of unequally spaced lines, which restrict the usefulness of the previously defined simple formulae, though they may still yield useful approximations. Even in these cases, though, the concept of maximum retardation is still a useful measure of the resolving power.

### 2.5. FOCAL LENGTH AND $f$ /NUMBER [\[top\]](#)

For gratings (or grating systems) that image as well as diffract light, or



disperse light that is not collimated, a *focal length* may be defined. If the beam diffracted from a grating of a given wavelength  $\lambda$  and order  $m$  converges to a focus, then the distance between this focus and the grating center is the focal length  $r'(\lambda)$ . [If the diffracted light is collimated, and then focused by a mirror or lens, the focal length is that of the refocusing mirror or lens and not the distance to the grating.] If the diffracted light is diverging, the focal length may still be defined, although by convention we take it to be negative (indicating that there is a virtual image behind the grating). Similarly, the incident light may diverge toward the grating (so we define the incidence or entrance slit distance  $r(\lambda) > 0$ ) or it may converge toward a focus behind the grating (for which  $r(\lambda) < 0$ ). Usually gratings are used in configurations for which  $r$  does not depend on wavelength (though in such cases  $r'$  usually depends on  $\lambda$ ).

In Figure 2-7, a typical concave grating configuration is shown; the monochromatic incident light (of wavelength  $\lambda$ ) diverges from a point source at A and is diffracted toward B. Points A and B are distances  $r$  and  $r'$ , respectively, from the grating center O. In this figure, both  $r$  and  $r'$  are positive.

Calling the width (or diameter) of the grating (in the dispersion plane)  $W$  allows the *input* and *output f/numbers* (also called *focal ratios*) to be defined:

$$f/\text{no}_{\text{INPUT}} = \frac{r}{W}, \quad f/\text{no}_{\text{OUTPUT}} = \frac{r'(\lambda)}{W} \quad (2-20)$$

Usually the input *f/number* is matched to the *f/number* of the light cone leaving the entrance optics (*e.g.*, an entrance slit or fiber) in order to use as much of the grating surface for diffraction as possible. This increases the amount of diffracted energy while not overfilling the grating (which would generally contribute to stray light).

For oblique incidence or diffraction, Eqs. (2-20) are often modified by replacing  $W$  with the projected width of the grating:

$$f/\text{no}_{\text{INPUT}} = \frac{r}{W \cos \alpha}, \quad f/\text{no}_{\text{OUTPUT}} = \frac{r'(\lambda)}{W \cos \beta} \quad (2-21)$$

These equations account for the reduced width of the grating as seen by the entrance and exit slits; moving toward oblique angles (*i.e.*, increasing  $|\alpha|$  or  $|\beta|$

) decreases the projected width and therefore increases the  $f$ /number.

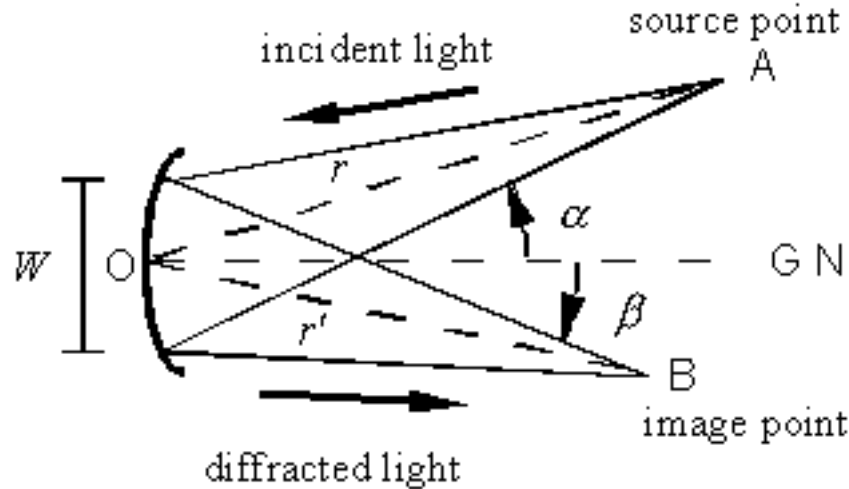


Figure 2-7. Geometry for focal distances and focal ratios ( $f$ /numbers). GN is the grating normal (perpendicular to the grating at its center, O),  $W$  is the width of the grating (its dimension perpendicular to the groove direction, which is out of the page), and A and B are the source and image points, respectively.

The focal length is an important parameter in the design and specification of grating spectrometers, since it governs the overall size of the optical system (unless folding mirrors are used). The ratio between the input and output focal lengths determines the projected width of the entrance slit that must be matched to the exit slit width or detector element size. The  $f$ /number is also important, as it is generally true that spectral aberrations decrease as  $f$ /number increases. Unfortunately, increasing the input  $f$ /number results in the grating subtending a smaller solid angle as seen from the entrance slit; this will reduce the amount of light energy the grating collects and consequently reduce the intensity of the diffracted beams. This trade-off prohibits the formulation of a simple rule for choosing the input and output  $f$ /numbers, so sophisticated design procedures have been developed to minimize aberrations while maximizing collected energy. See [Chapter 7](#) for a discussion of the imaging properties and [Chapter 8](#) for a description of the efficiency characteristics of grating systems.

## 2.6. ANAMORPHIC MAGNIFICATION [\[top\]](#)

For a given wavelength  $\lambda$ , we may consider the ratio of the width of a collimated diffracted beam to that of a collimated incident beam to be a measure of the effective magnification of the grating (see Figure 2-8). From this figure we see that this ratio is

$$\frac{b}{a} = \frac{\cos \beta}{\cos \alpha} \quad (2-22)$$

Since  $\alpha$  and  $\beta$  depend on  $\lambda$  through the grating equation (2-1), this magnification will vary with wavelength. The ratio  $b/a$  is called the *anamorphic magnification*; for a given wavelength  $\lambda$ , it depends only on the angular configuration in which the grating is used.

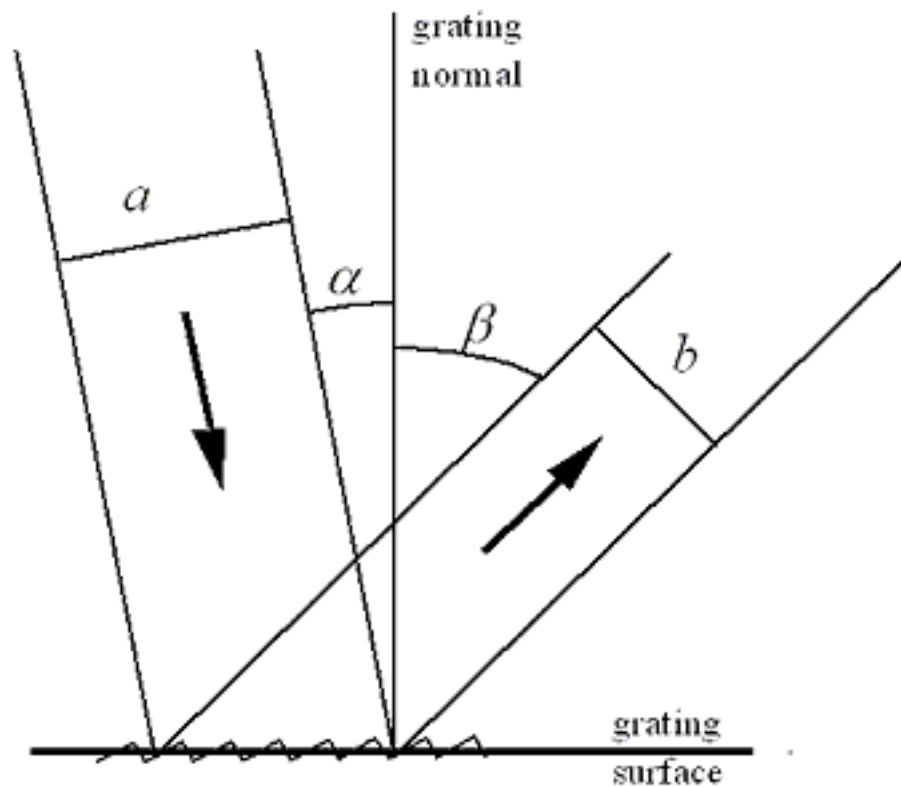


Figure 2-8. Anamorphic magnification. The ratio  $b/a$  of the beam widths equals the anamorphic magnification.

The magnification of an object not located at infinity (so that the incident rays are not collimated) is discussed in [Chapter 8](#).

## 2.7. FREE SPECTRAL RANGE [\[top\]](#)

For a given set of incidence and diffraction angles, the grating equation is satisfied for a different wavelength for each integral diffraction order  $m$ . Thus light of several wavelengths (each in a different order) will be diffracted along the same direction: light of wavelength  $\lambda$  in order  $m$  is diffracted along the same direction as light of wavelength  $\lambda/2$  in order  $2m$ , *etc.*

The range of wavelengths in a given spectral order for which superposition of light from adjacent orders does not occur is called the *free spectral range*  $F\lambda$ . It can be calculated directly from its definition: in order  $m$ , the wavelength of light that diffracts along the direction of  $\lambda_1$  in order  $m+1$  is  $\lambda_1 + \Delta\lambda$ , where

$$\lambda_1 + \Delta\lambda = \frac{m+1}{m} \lambda_1 \quad (2-23)$$

from which

$$F\lambda = \Delta\lambda = \frac{\lambda_1}{m} . \quad (2-24)$$

The concept of free spectral range applies to all gratings capable of operation in more than one diffraction order, but it is particularly important in the case of echelles, because they operate in high orders with correspondingly short free spectral ranges.

Free spectral range and order sorting are intimately related, since grating systems with greater free spectral ranges may have less need for filters (or cross-dispersers) that absorb or diffract light from overlapping spectral orders. This is one reason why first-order applications are widely popular.

## 2.8. ENERGY DISTRIBUTION (GRATING EFFICIENCY)

[\[top\]](#)

The distribution of incident field power of a given wavelength diffracted by a grating into the various spectral order depends on many parameters, including the power and polarization of the incident light, the angles of incidence and diffraction, the (complex) index of refraction of the metal (or glass or dielectric) of the grating, and the groove spacing. A complete treatment of grating efficiency requires the vector formalism of electromagnetic theory (*i.e.*, Maxwell's equations), which has been studied in detail over the past few decades. While the theory does not yield conclusions easily, certain rules of thumb can be useful in making approximate predictions. The topic of grating efficiency is addressed more fully in [Chapter 9](#).

Recently, computer codes have become commercially available that accurately predict grating efficiency for a wide variety of groove profiles over wide spectral ranges.

## 2.9. SCATTERED AND STRAY LIGHT [\[top\]](#)

All light that reaches the image plane from anywhere other than the grating, by any means other than diffraction as governed by Eq. (2-1), is called *stray light*. All components in an optical system contribute stray light, as will any baffles, apertures, and partially reflecting surfaces. Unwanted light originating from the grating itself is often called *scattered light*.

### 2.9.1. Scattered light

Of the radiation incident on the surface of a diffraction grating, some will be diffracted according to Eq. (2-1) and some will be absorbed by the grating itself. The remainder is unwanted energy called *scattered light*. Scattered light may arise from several factors, including imperfections in the

shape and spacing of the grooves and roughness on the surface of the grating.

*Diffuse scattered light* is scattered into the hemisphere in front of the grating surface. It is due mainly to grating surface microroughness. It is the primary cause of scattered light in interference gratings. For monochromatic light incident on a grating, the intensity of diffuse scattered light is higher near the diffraction orders for that wavelength than between the diffracted orders. M.C. Hutley (National Physical Laboratory) found this intensity to be proportional to slit area, and probably proportional to  $1/\lambda^4$ .

*In-plane scatter* is unwanted energy in the dispersion plane. Due primarily to random variations in the groove spacing or groove depth, its intensity is directly proportional to slit area and probably inversely proportional to the square of the wavelength.

*Ghosts* are caused by periodic errors in the groove spacing. Characteristic of ruled gratings, interference gratings are free from ghosts when properly made.

### 2.9.2. Instrumental stray light

Stray light for which the grating cannot be blamed is called *instrumental stray light*. Most important is the ever-present light reflected into the zero order, which must be trapped so that it does not contribute to stray light. Light diffracted into other orders may also find its way to the detector and therefore constitute stray light. Diffraction from sharp edges and apertures causes light to propagate along directions other than those predicted by the grating equation. Reflection from instrument chamber walls and mounting hardware also contributes to the redirection of unwanted energy toward the image plane; generally, a smaller instrument chamber presents more significant stray light problems. Light incident on detector elements may be reflected back toward the grating and rediffracted; since the angle of incidence may now be different, light rediffracted along a given direction will generally be of a different wavelength than the light that originally diffracted along the same direction. Baffles, which trap diffracted energy outside the spectrum of interest, are intended to reduce the amount of light in other orders and in other wavelengths, but they may themselves diffract and reflect this light so that it ultimately

reaches the image plane.

## 2.10. SIGNAL-TO-NOISE RATIO (SNR) [\[top\]](#)

The *signal-to-noise ratio* (SNR) is the ratio of diffracted energy to unwanted light energy. While we might be tempted to think that increasing diffraction efficiency will increase SNR, stray light usually plays the limiting role in the achievable SNR for a grating system.

Replicated gratings from ruled master gratings generally have quite high SNRs, though holographic gratings sometimes have even higher SNRs, since they have no ghosts due to periodic errors in groove location and lower interorder stray light.

As SNR is an instrument function, not a property of the grating only, there exist no clear rules of thumb regarding what type of grating will provide higher SNR.

[PREVIOUS CHAPTER](#)   [NEXT CHAPTER](#)

[Back to top](#)

# 6. PLANE GRATINGS AND THEIR MOUNTS

---

PREVIOUS CHAPTER  
NEXT CHAPTER

Copyright 2002, Thermo RGL,  
All Rights Reserved

## TABLE OF CONTENTS

- 6.1. GRATING MOUNT TERMINOLOGY
- 6.2. PLANE GRATING MONOCHROMATOR MOUNTS
  - 6.2.1. *The Czerny-Turner Monochromator*
  - 6.2.2. *The Ebert-Fastie Monochromator*
  - 6.2.3. *The Monk-Gillieson Monochromator*
  - 6.2.4. *The Littrow Mount*
  - 6.2.5. *Double & Triple Monochromators*

## **6.1. GRATING MOUNT TERMINOLOGY** [\[top\]](#)

The auxiliary collimating and focusing optics that modify the wavefronts incident on and diffracted by a grating, as well as the angular configuration in which it is used, is called its *mount*. Grating mounts are a class of *spectrometer*, a term which usually refers to any spectroscopic instrument, regardless of whether it scans wavelengths individually or entire spectra simultaneously, or whether it employs a prism or grating. For this discussion we consider grating spectrometers only.

A *monochromator* is a spectrometer that images a single wavelength or wavelength band at a time onto an exit slit; the spectrum is scanned by the relative motion of the entrance (and/or exit) optics (usually slits) with respect to the grating. A *spectrograph* is a spectrometer that images a range of wavelengths simultaneously, either onto photographic film or a series of detector elements, or through several exit slits (sometimes called a



*polychromator*). The defining characteristic of a spectrograph is that an entire section of the spectrum is recorded at once.

## 6.2. PLANE GRATING MONOCHROMATOR MOUNTS

[\[top\]](#)

A *plane grating* is one whose surface is flat. Plane gratings are normally used in collimated incident light, which is dispersed by wavelength but do not focused. These mounts require auxiliary optics, such as lenses or mirrors, to collect and focus the energy. Some simplified plane grating mounts illuminate the grating with converging light, though the focal properties of the system will then depend on wavelength. For simplicity, only plane reflection grating mounts are discussed below, though each mount may have a transmission grating analogue.

### 6.2.1. The Czerny-Turner Monochromator

This design involves a classical plane grating illuminated by collimated light. The incident light is usually diverging from a source or slit, and collimated by a concave mirror (the *collimator*), and the diffracted light is focused by a second concave mirror (the *camera*); see Figure 6-1. Ideally, since the grating is planar and classical, and used in collimated incident light, no aberrations should be introduced into the diffracted wavefronts. In practice, aberrations are contributed by the off-axis use of the concave spherical mirrors.

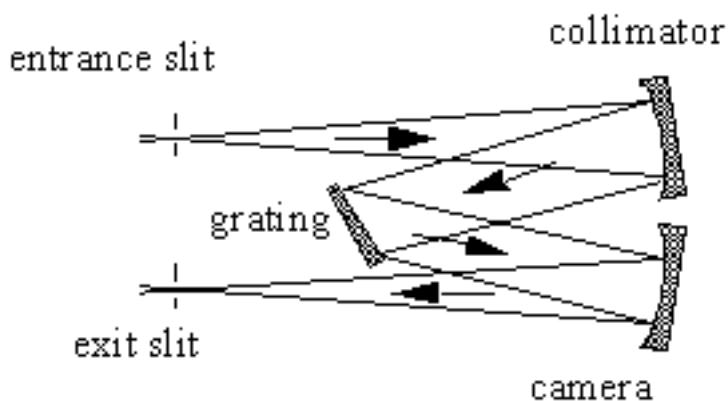


*Figure 6-1. The Czerny-Turner mount.* The plane grating provides dispersion and the concave mirrors provide focusing.

---

Like all monochromator mounts, the wavelengths are imaged individually. The spectrum is scanned by rotating the grating; this moves the grating normal relative to the incident and diffracted beams, which (by Eq. (2-1)) changes the wavelength diffracted toward the camera. For a Czerny-Turner monochromator, light incident and diffracted by the grating is collimated, so the spectrum remains at focus at the exit slit for each wavelength, since only the grating can introduce wavelength-dependent focusing properties.

Aberrations caused by the auxiliary mirrors include astigmatism and spherical aberration (each of which is contributed additively by the mirrors); as with all concave mirror geometries, astigmatism increases as the angle of reflection increases. Coma, though generally present, can be eliminated at one wavelength through proper choice of the angles of reflection at the mirrors; due to the anamorphic (wavelength-dependent) tangential magnification of the grating, the images of the other wavelengths experience subsidiary coma (which becomes troublesome only in special systems).

### **6.2.2. The Ebert-Fastie Monochromator**

This design is a special case of a Czerny-Turner mount in which a single relatively large concave mirror serves as both the collimator and the camera (Fig. 6-2). Its use is limited, since stray light and aberrations are difficult to control.

---

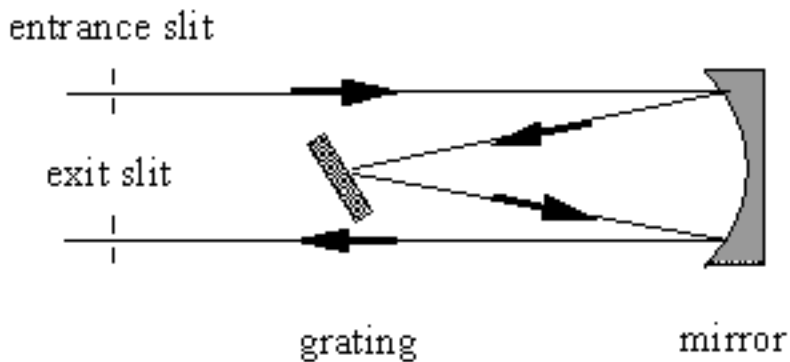


*Figure 6-2. The Ebert-Fastie mount. A single concave mirror replaces the two concave mirrors found in Czerny-Turner mounts.*

---

### 6.2.3. The Monk-Gillieson Monochromator

In this mount (see Figure 6-3), a plane grating is illuminated by converging light ( $r < 0$ ). Usually light diverging from an entrance slit (or fiber) is rendered converging by off-axis reflection from a concave mirror (which introduces aberrations, so the light incident on the grating is not composed of perfectly spherical converging wavefronts). The grating diffracts the light, which converges toward the exit slit; the spectrum is scanned by rotating the grating to bring different wavelengths into focus at or near the exit slit. Often the angles of reflection (from the primary mirror), incidence and diffraction are small (measured from the appropriate surface normals), which keeps aberrations (especially off-axis astigmatism) to a minimum.

---

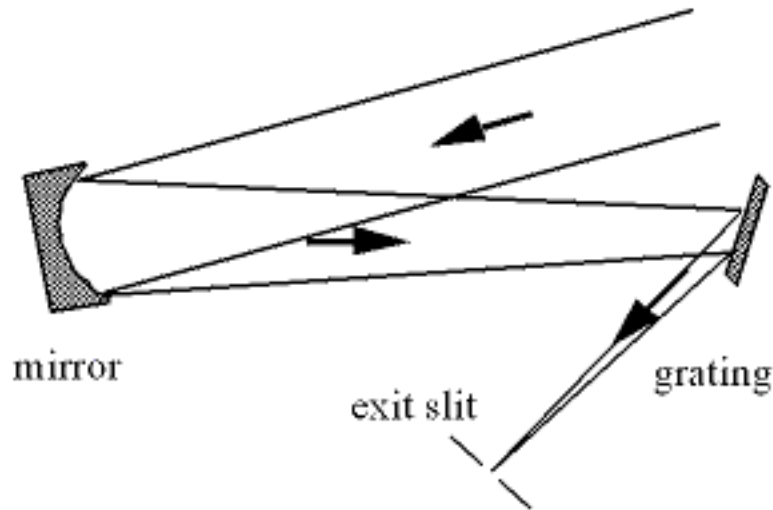


Figure 6-3. *The Monk-Gillieson mount.* A plane grating is used in converging light.

---

Since the incident light is not collimated, the grating introduces wavelength-dependent aberrations into the diffracted wavefronts (see [Chapter 7](#)). Consequently the spectrum cannot remain in focus at a fixed exit slit when the grating is rotated (unless this rotation is about an axis displaced from the central groove of the grating, as pointed out by Schroeder<sup>5</sup>). For low-resolution applications, the Monk-Gillieson mount enjoys a certain amount of popularity, since it represents the simplest and least expensive spectrometric system imaginable.

#### 6.2.4. The Littrow Mount

A grating used in the Littrow or autocollimating configuration diffracts light of wavelength  $\lambda$  back along the incident light direction (Fig. 6-4). In a *Littrow monochromator*, the spectrum is scanned by rotating the grating; this reorients the grating normal, so the angles of incidence  $\alpha$  and diffraction  $\beta$  change (even though  $\alpha = \beta$  for all  $\lambda$ ). The same auxiliary optics can be used as both

---

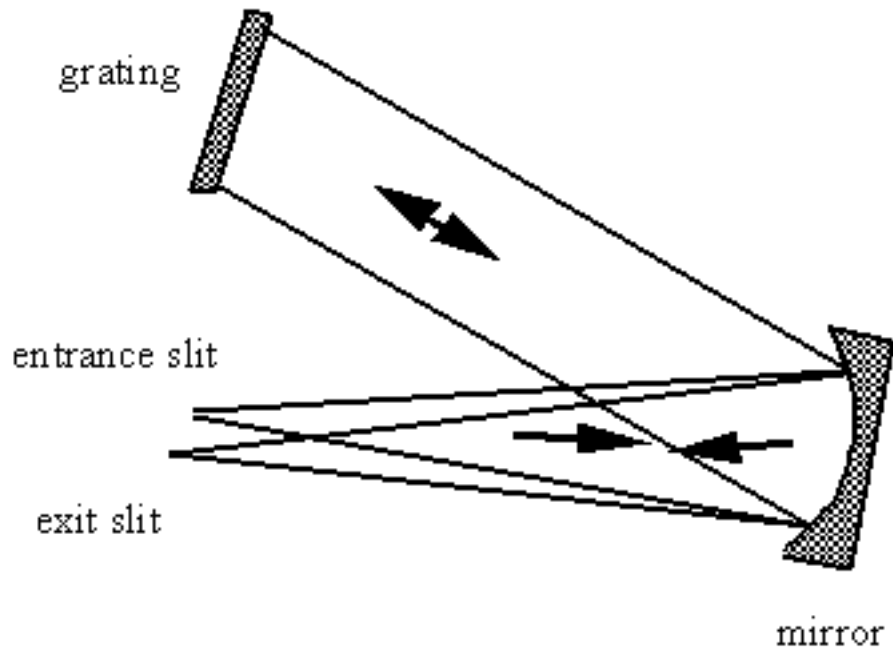


*Figure 6-4. The Littrow monochromator mount. The entrance and exit slits are slightly above and below the dispersion plane, respectively; they are shown separated for clarity.*

---

collimator and camera, since the diffracted rays retrace the incident rays. Usually the entrance slit and exit slit (or image plane) will be offset slightly along the direction parallel to the grooves so that they do not coincide; of course, this will generally introduce out-of-plane aberrations. As a result, true Littrow monochromators are quite popular in laser tuning applications (see [Chapter 12](#)).

### 6.2.5. Double & Triple Monochromators

Two monochromator mounts used in series form a *double monochromator*. The exit slit of the first monochromator usually serves as the entrance slit for the second monochromator (see [Figure 6-5](#)). Stray light in a double

---

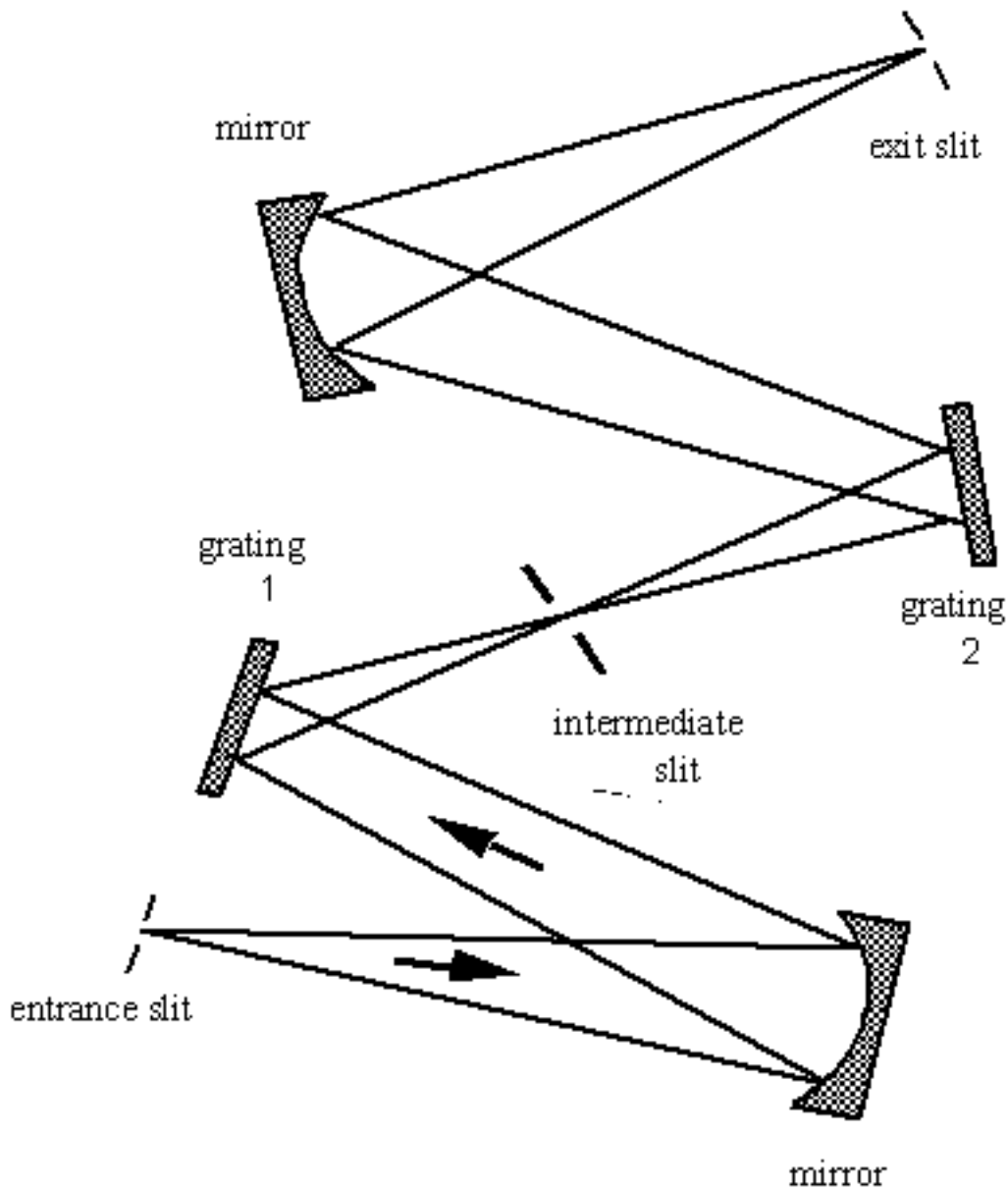


Figure 6-5. A double monochromator mount.

monochromator is much lower than in a single monochromator: it is the product of ratios of stray light intensity to parent line intensity for each system. Also, the reciprocal linear dispersion of the entire system is the sum of the reciprocal linear dispersions of each monochromator.

A *triple monochromator* mount consists of three monochromators in series. These mounts are used only when the demands to reduce stray light are extraordinarily severe (*e.g.*, Raman spectroscopy).

[PREVIOUS CHAPTER](#)   [NEXT CHAPTER](#)

[\*Back to top\*](#)

# 9. EFFICIENCY CHARACTERISTICS OF DIFFRACTION GRATINGS

---

[PREVIOUS CHAPTER](#)

[NEXT CHAPTER](#)

[Copyright 2002, Thermo RGL,](#)

[All Rights Reserved](#)

## [TABLE OF CONTENTS](#)

### [9.0. INTRODUCTION](#)

#### [9.1. GRATING EFFICIENCY AND GROOVE SHAPE](#)

#### [9.2. EFFICIENCY CHARACTERISTICS FOR TRIANGULAR-GROOVE GRATINGS](#)

#### [9.3. EFFICIENCY CHARACTERISTICS FOR SINUSOIDAL-GROOVE GRATINGS](#)

#### [9.4. THE EFFECTS OF FINITE CONDUCTIVITY](#)

#### [9.5. DISTRIBUTION OF ENERGY BY DIFFRACTION ORDER](#)

#### [9.6. USEFUL WAVELENGTH RANGE](#)

#### [9.7. BLAZING OF RULED TRANSMISSION GRATINGS](#)

#### [9.8. BLAZING OF HOLOGRAPHIC REFLECTION GRATINGS](#)

#### [9.9. OVERCOATING OF REFLECTION GRATINGS](#)

## **9.0. INTRODUCTION** [\[top\]](#)

Efficiency and its variation with wavelength and spectral order are important characteristics of a diffraction grating. For a reflection grating, efficiency is defined as the energy flow (power) of monochromatic light diffracted into the order being measured, relative either to the energy flow of the incident light (*absolute efficiency*) or to the energy flow of specular reflection from a polished mirror substrate coated with the same material (*relative efficiency*). Efficiency is defined similarly for transmission gratings, except that an uncoated substrate is used in the measurement of relative efficiency.

High-efficiency gratings are desirable for several reasons. A grating with high efficiency is more useful than one with lower efficiency in measuring weak transition lines in optical spectra. A grating with high efficiency may allow the reflectivity and transmissivity specifications for the other components in the spectrometer to be relaxed. Moreover, higher diffracted energy may imply lower instrumental stray light due to other diffracted orders, as the total energy flow for a given



wavelength leaving the grating is conserved (being equal to the energy flow incident on it minus any scattering and absorption).

Control over the magnitude and variation of diffracted energy with wavelength is called *blazing*, and it involves the manipulation of the micro-geometry of the grating grooves. In the 1888 edition of *Encyclopædia Britannica*, Lord Rayleigh recognized that the energy flow distribution (by wavelength) of a diffraction grating could be altered by modifying the shape of the grating grooves. A few decades later, R.W. Wood showed this to be true when he ruled a grating on which he had controlled the groove shape, thereby producing the first deliberately blazed diffraction grating.

The choice of an optimal efficiency curve for a grating depends on the specific application. Often the desired instrumental efficiency is linear; that is, the intensity of light transformed into signal at the image plane must be constant across the spectrum. To approach this as closely as possible, the spectral emissivity of the light source and the spectral response of the detector should be considered, from which the desired grating efficiency curve can be derived. Usually this requires peak grating efficiency in the region of the spectrum where the detectors are least sensitive; for example, a visible-light spectrometer using a silicon detector would be much less sensitive in the blue than in the red, suggesting that the grating itself be blazed to yield a peak efficiency in the blue.

A typical *efficiency curve* (a plot of absolute or relative diffracted efficiency vs. diffracted wavelength  $\lambda$ ) is shown in Figure 9-1. Usually such a curve shows

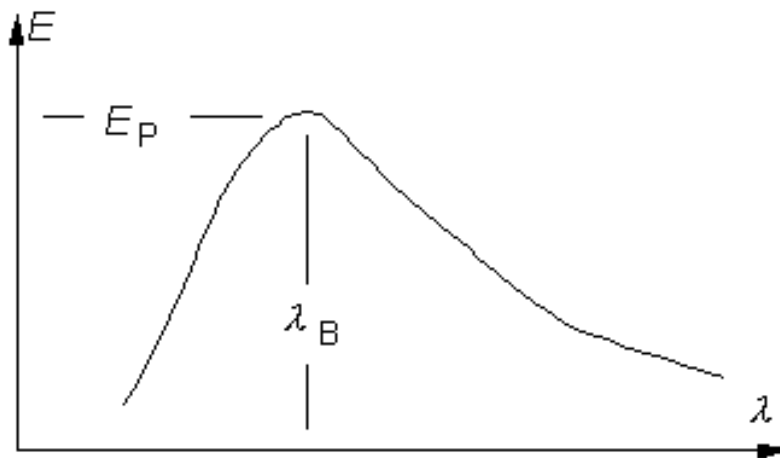


Figure 9-1. A typical (simplified) efficiency curve. This curve shows the efficiency  $E$  of a grating in a given spectral order  $m$ , measured vs. the diffracted wavelength  $\lambda$ . The peak efficiency  $E_p$  occurs at the blaze wavelength  $\lambda_B$ .

a single maximum, at the *peak wavelength* (or *blaze wavelength*)  $\lambda_B$ . This curve corresponds to a

given diffraction order  $m$ ; the peak of the curve decreases in magnitude and shifts toward shorter wavelengths as  $|m|$  increases. The efficiency curve also depends on the angles of use (*i.e.*, the angles of incidence and diffraction). Moreover, the curve depends on the groove spacing  $d$  (more appropriately, on the dimensionless parameter  $\lambda/d$ ) and the material with which the grating is coated (for reflection gratings) or made (for transmission gratings).

In many instances the diffracted power depends on the polarization of the incident light. *P-plane* or *TE polarized light* is polarized parallel to the grating grooves, while *S-plane* or *TM polarized light* is polarized perpendicular to the grating grooves (see Figure 9-2). For completely unpolarized incident light, the efficiency curve will be exactly halfway between the P and S efficiency curves.

Usually light from a single spectral order  $m$  is used in a spectroscopic instrument, so a grating with ideal efficiency characteristics would diffract all of the power incident on it into this order (for the wavelength range considered). In practice, this is never true: the distribution of the power by the grating depends in a complicated way on the groove spacing and profile, the spectral order, the wavelength, and the grating material.

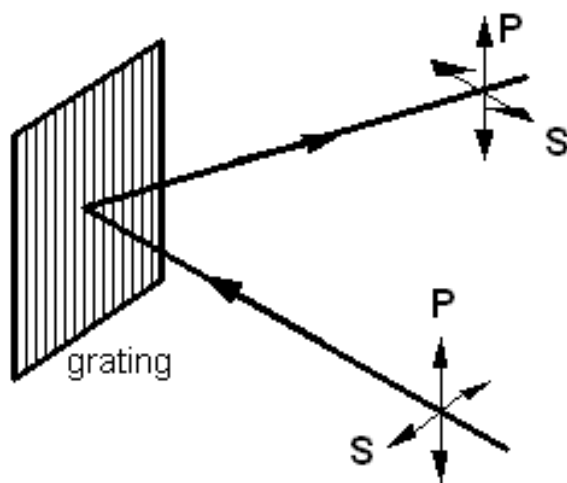


*Figure 9-2. S and P polarizations* The P polarization components of the incident and diffracted beams are polarized parallel to the grating grooves; the S components are polarized perpendicular to the P components. Both the S and P components are perpendicular to the propagation directions.

*Anomalies* are locations on an efficiency curve (efficiency plotted vs. wavelength) at which the efficiency changes abruptly. First observed by R. W. Wood, these sharp peaks and troughs in an efficiency curve are sometimes referred to as Wood's anomalies. Anomalies are rarely observed in P polarization efficiency curves, but they are often seen in S polarization curves (see Figure 9-3).

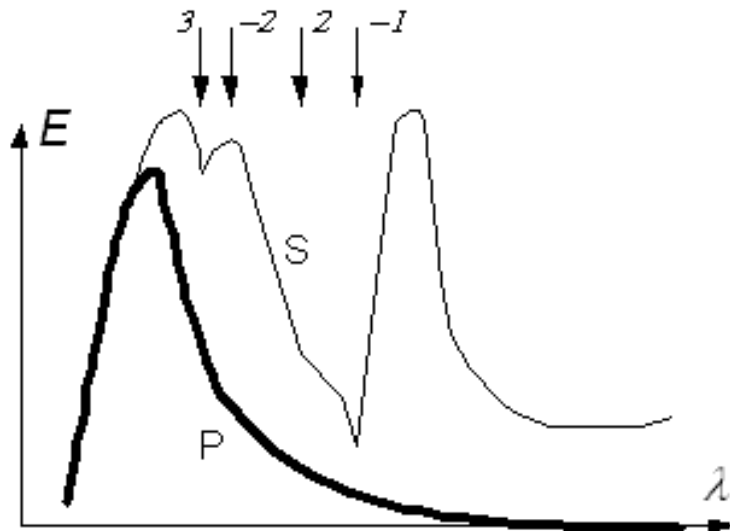


Figure 9-3. Anomalies in the first order for a typical grating with triangular grooves. The P efficiency curve (thick line) is smooth, but anomalies are evident in the S curve (thin line). The passing-off locations are identified by their spectral order at the top of the figure.

Lord Rayleigh predicted the locations (in the spectrum) where such anomalies would be found: he suggested that anomalies occur when light of a given wavelength  $\lambda'$  and spectral order  $m'$  is diffracted at  $|\beta| = 90^\circ$  from the grating normal (*i.e.*, it passes over the grating horizon). For wavelengths  $\lambda < \lambda'$ ,  $|\beta| < 90^\circ$ , so diffraction is possible in order  $m'$  (and all lower orders), but for  $\lambda > \lambda'$  no diffraction is possible in order  $m'$  (but it is still possible in lower orders). Thus there is a discontinuity in the diffracted power *vs.*  $\lambda$  in order  $m'$  at wavelength  $\lambda$ , and the power that would diffract into this order for  $\lambda > \lambda'$  is redistributed among the other spectral orders. This causes abrupt changes in the power diffracted into these other orders.

The Rayleigh explanation does not cover the extension towards longer wavelengths, where anomalies are due to resonance effects. The position of an anomaly depends to some degree on the optical constants of the reflecting material of the grating surface.

## 9.1. GRATING EFFICIENCY AND GROOVE SHAPE [\[top\]](#)

The maximum efficiency of a grating is typically obtained with a simple smooth triangular groove profile, as shown in Figure 9-4, when the groove (or

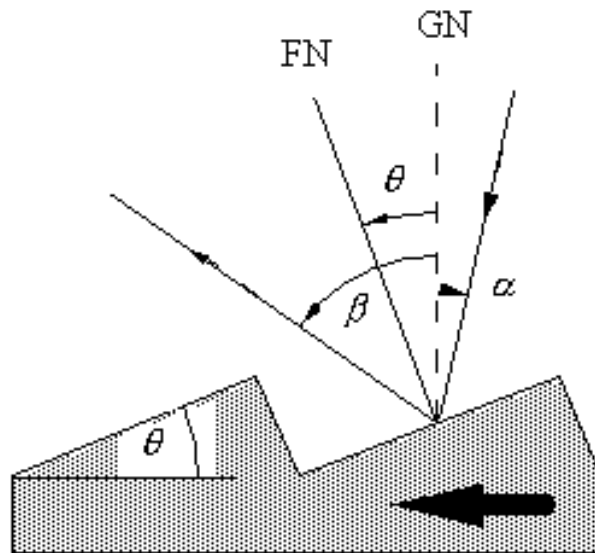


*Figure 9-4. Triangular groove geometry.* The angles of incidence  $\alpha$  and diffraction  $\beta$  are shown in relation to the facet angle  $\theta$  for the blaze condition. GN is the grating normal and FN is the facet normal. The facet normal bisects the angle between the incident and diffracted rays. The blaze arrow (shown) points from GN to FN.

blaze) angle  $\theta$  is such that the specular reflection angle for the angle of incidence is equal (in magnitude and opposite in sign) to the angle of diffraction. Ideally, the groove facet should be flat with smooth straight edges, and be generally free from irregularities on a scale comparable to the small fraction ( $< 1/10$ ) of the wavelength of light being diffracted.

Fraunhofer was well aware that the distribution of power among the various diffraction orders depended on the shape of the individual grating grooves. Wood, many decades later, was the first to achieve a degree of control over the groove shape, thereby concentrating spectral energy into one angular region. Wood's gratings were seen to light up, or 'blaze', when viewed at the correct angle.

## 9.2. EFFICIENCY CHARACTERISTICS FOR TRIANGULAR-GROOVE GRATINGS [\[top\]](#)

Gratings with triangular grooves can be generated by mechanical ruling, or by blazing sinusoidal groove profiles by ion etching. The efficiency behavior of gratings with triangular groove profiles (*i.e.*, blazed gratings) may be divided into six families, depending on the blaze angle:<sup>9</sup>

<i>family</i>	<i>blaze angle</i>
very low blaze angle	$\theta < 5^\circ$
low blaze angle	$5^\circ < \theta < 10^\circ$
medium blaze angle	$10^\circ < \theta < 18^\circ$
special low anomaly	$18^\circ < \theta < 22^\circ$
high blaze angle	$22^\circ < \theta < 38^\circ$
very high blaze angle	$\theta > 38^\circ$

*Very low blaze angle* gratings ( $\theta < 5^\circ$ ) exhibit efficiency behavior that is almost perfectly scalar; that is, polarization effects are virtually nonexistent. In this region, a simple picture of blazing is applicable, in which each groove facet can be considered a simple flat mirror. The diffracted efficiency is greatest for that wavelength that is diffracted by the grating in the same direction as it would be reflected by the facets. This efficiency peak occurs at  $\lambda/d = 2 \sin\theta$  (provided the angle between the incident and diffracted beams is not excessive). At  $\lambda_B/2$ , where  $\lambda_B$  is the blaze wavelength, the diffracted efficiency will be virtually zero (Figure 9-5) since for this wavelength the second-order efficiency will be at its peak. Fifty-percent absolute efficiency is obtained from roughly  $0.67\lambda_B$  to  $1.8\lambda_B$ .

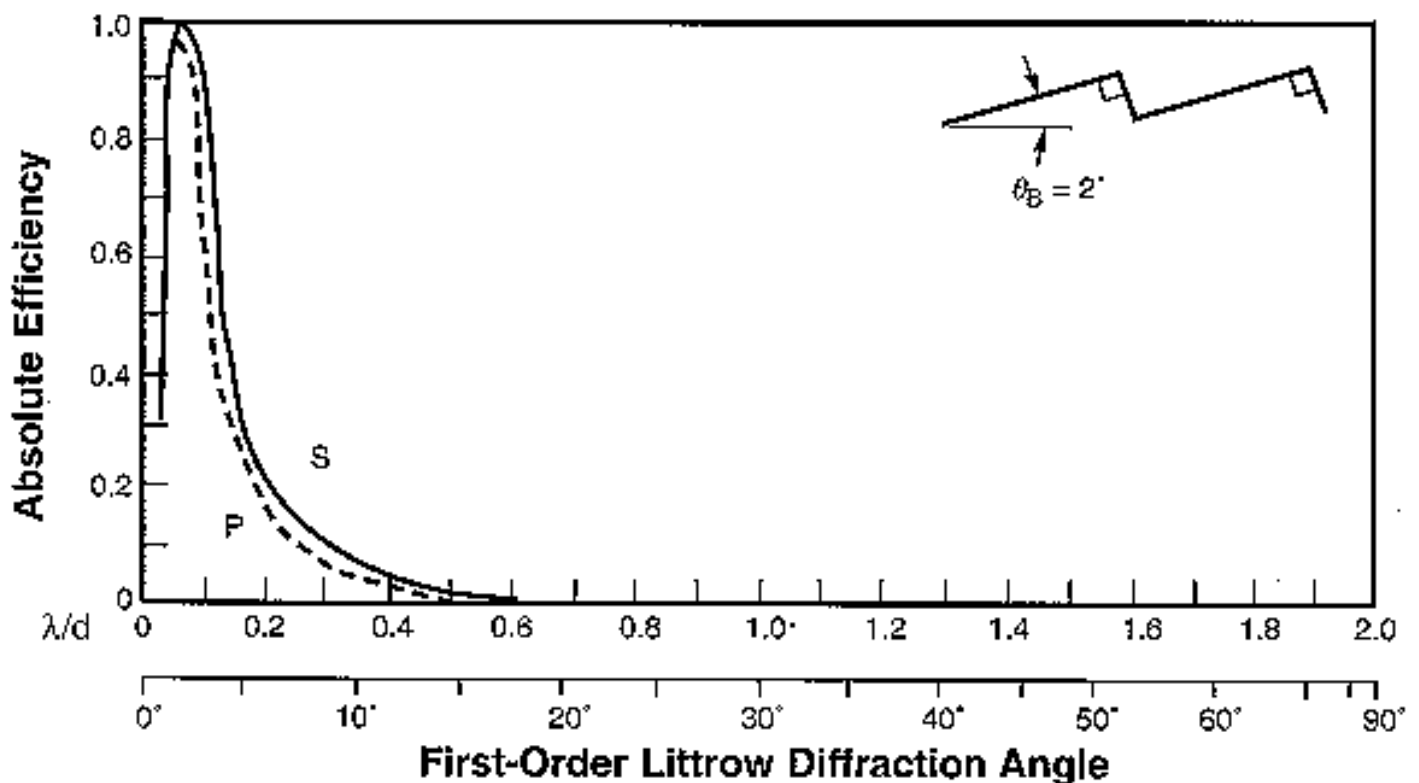


Figure 9-5. First-order theoretical efficiency curve:  $2^\circ$  blaze angle and Littrow mounting ( $2K = 0$ ). Solid curve, S-plane; dashed curve, P-plane.

For *low blaze angle* gratings ( $5^\circ < \theta < 10^\circ$ ), polarization effects will occur within their usable range (see Figure 9-6). In particular, a strong anomaly is seen near  $\lambda/d = 2/3$ . Also observed is the theoretical S-plane theoretical efficiency peak of 100% exactly at the nominal blaze, combined with a P-plane peak that is lower and at a shorter wavelength. It is characteristic of all P-plane curves to decrease monotonically from their peak toward zero as  $\lambda/d \rightarrow 2$ , beyond which diffraction is not possible (see Eq. (2-1)). Even though the wavelength band over which 50% efficiency is attained in unpolarized light is from  $0.67\lambda_B$  to  $1.8\lambda_B$ , gratings of this type (with 1200 groove per millimeter, for example) are widely used, because they most effectively cover the wavelength range between 200 and 800 nm (in which most ultraviolet-visible (U5-Vis) spectrophotometers operate).

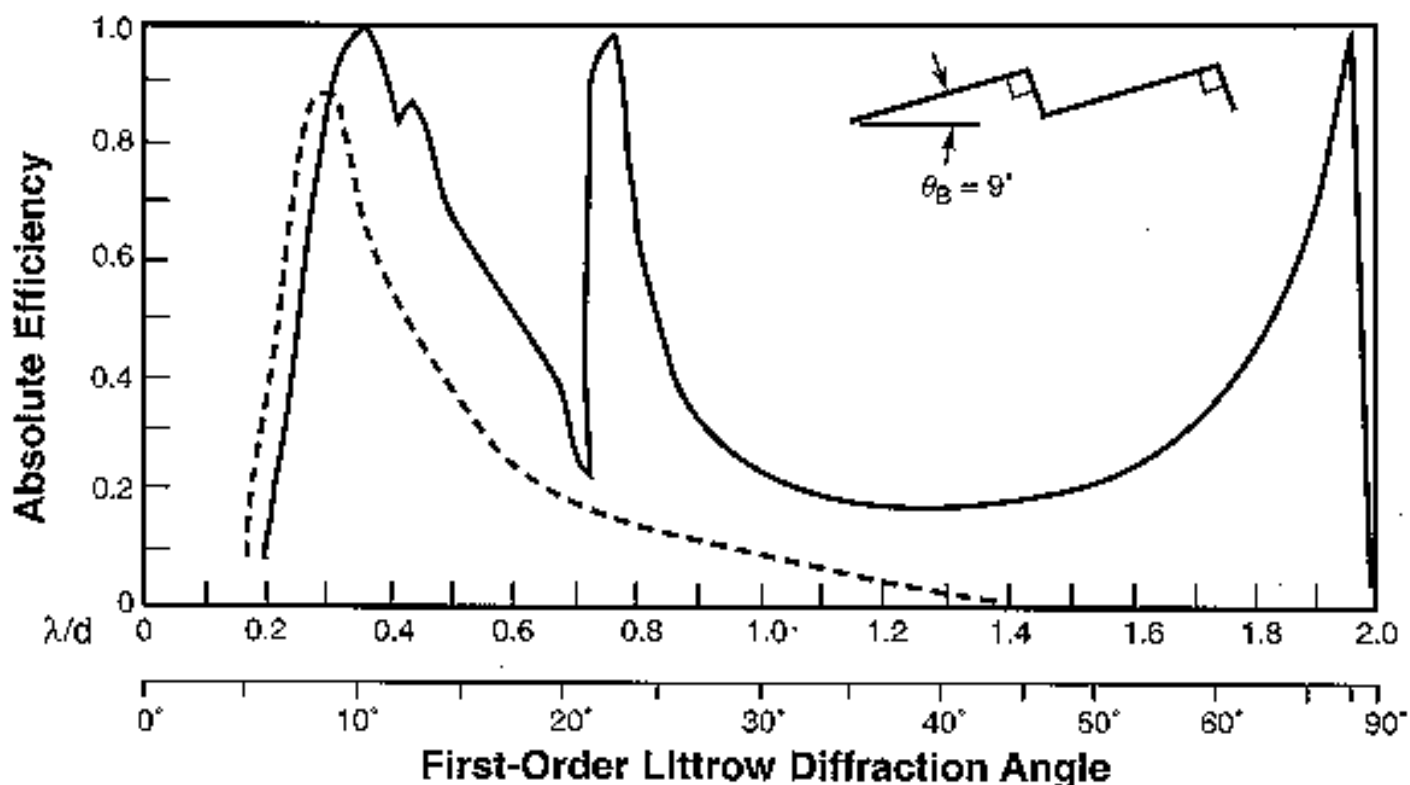


Figure 9-6. Same as Figure 9-5, except  $9^\circ$  blaze angle.

A typical efficiency curve for a *medium blaze angle* grating ( $10^\circ < \theta < 18^\circ$ ) is shown in Figure 9-7. As a reminder that for unpolarized light the efficiency is simply the arithmetic average of the S- and P-plane efficiencies, such a curve is shown in this figure only, to keep the other presentations simple.

The *low-anomaly blaze angle* region ( $18^\circ < \theta < 22^\circ$ ) is a special one. Due to the fact that the strong anomaly that corresponds to the -1 and +2 orders passing off ( $\lambda/d = 2/3$ ) occurs just where

these gratings have their peak efficiency, this anomaly ends up being severely suppressed (Figure 9-8). This property is quite well maintained over a large range of angular deviations (the angle between the incident and diffracted beams), namely up to  $25^\circ$ , but it depends on the grooves having an apex angle near  $90^\circ$ . The relatively low P-plane efficiency of this family of blazed gratings holds the 50% efficiency band from  $0.7\lambda_B$  to  $1.9\lambda_B$ .

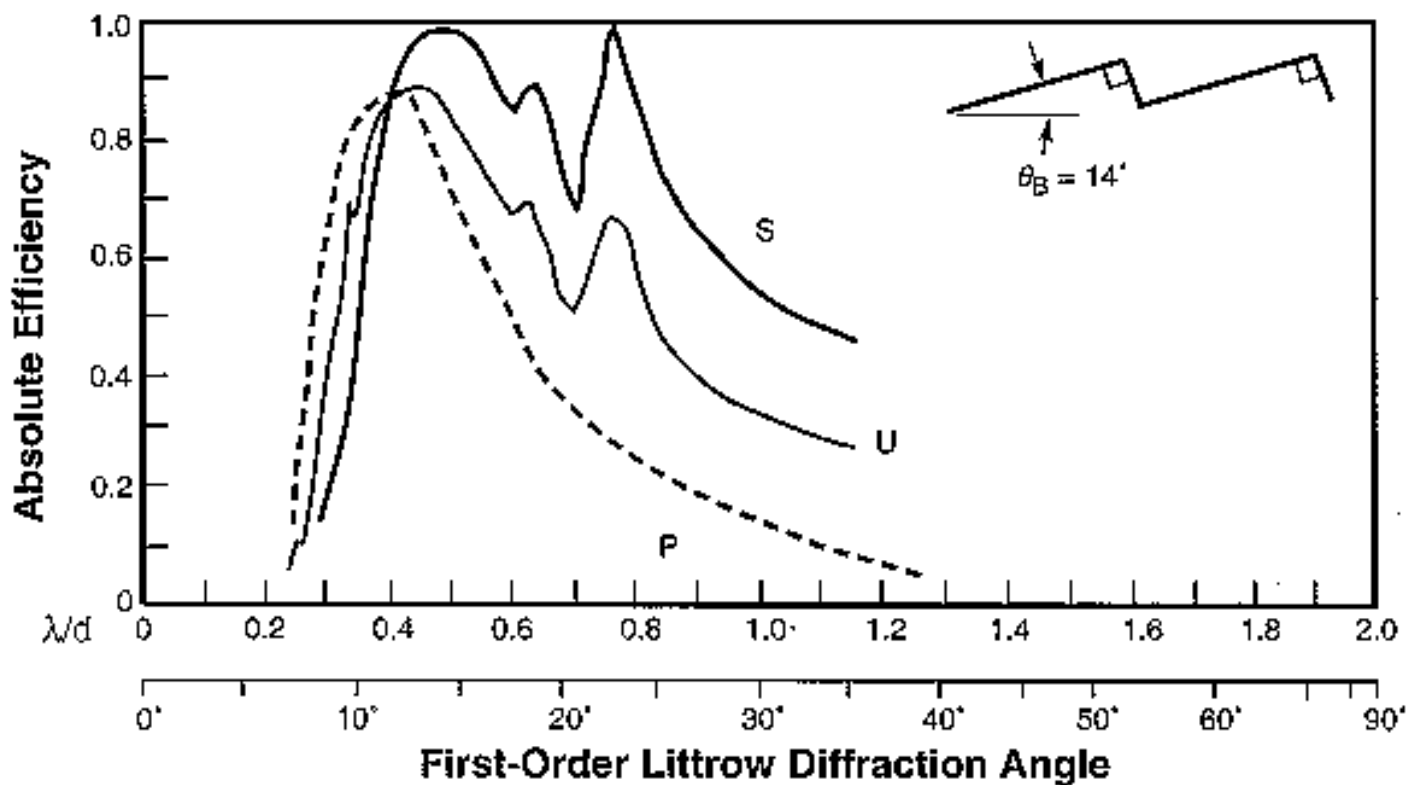


Figure 9-7. Same as Figure 9-5, except  $14^\circ$  blaze angle. The curve for unpolarized light (marked U) is also shown; it lies exactly halfway between the S and P curves.

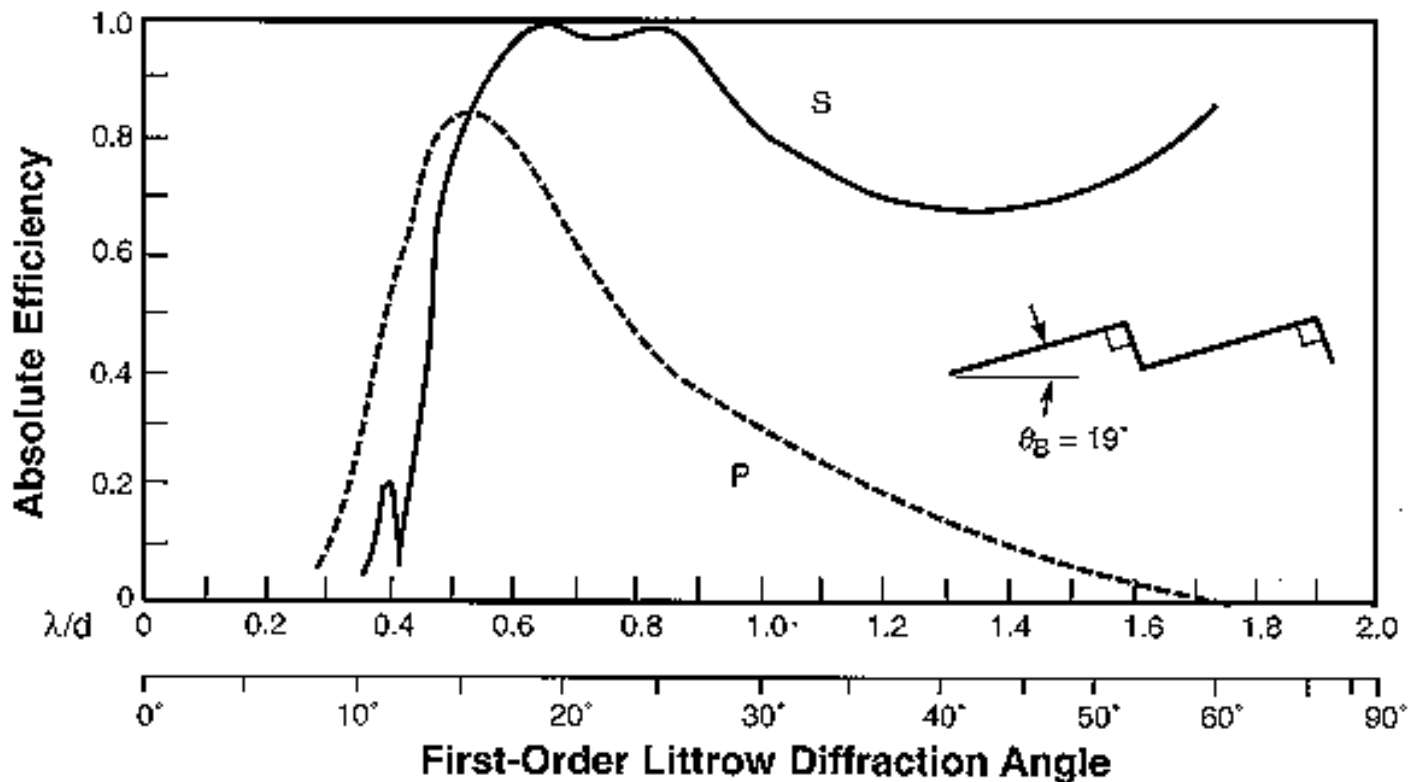


Figure 9-8. Same as Figure 9-5, except  $19^\circ$  blaze angle.

*High blaze angle* gratings ( $22^\circ < \theta < 38^\circ$ ) are widely used, despite the presence of a very strong anomaly in their efficiency curves (Figure 9-9). For unpolarized light, the effect of this anomaly is greatly attenuated by its coincidence with the P-plane peak. Another method for reducing anomalies for such gratings is to use them at angular deviations above  $45^\circ$ , although this involves some sacrifice in efficiency and wavelength range. The 50% efficiency is theoretically attainable in the Littrow configuration from  $0.6\lambda_B$  to  $2\lambda_B$ , but in practice the long-wavelength end corresponds to such an extreme angle of diffraction that instrumental difficulties arise.



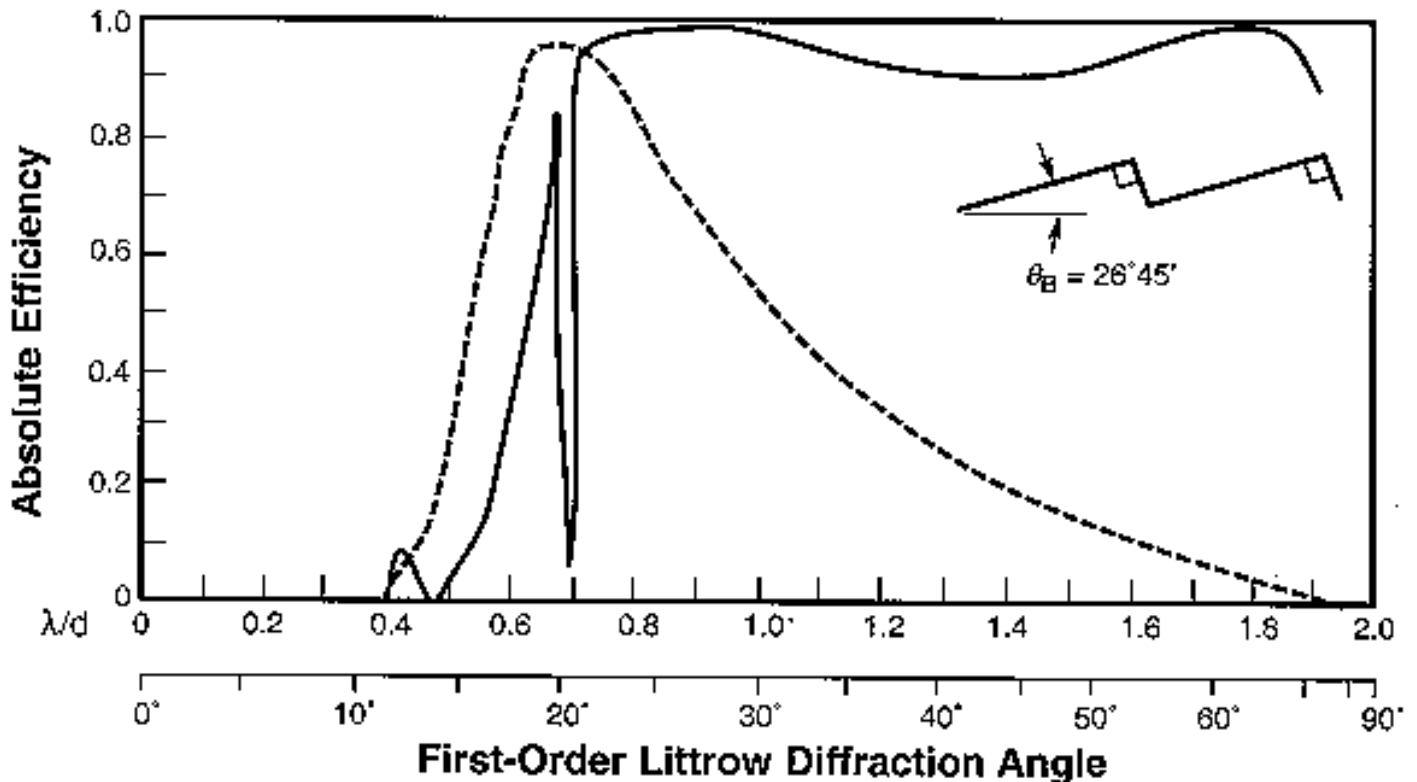


Figure 9-9. Same as Figure 9-5, except  $26^{\circ} 45'$  blaze angle.

Theoretically, all gratings have a second high-efficiency peak in the S-plane at angles corresponding to the complement of the blaze angle ( $90^{\circ} - \theta$ ); in practice, this peak is fully developed only on steeper groove-angle gratings, and then only when the steep face of the groove is not too badly deformed by the lateral plastic flow inherent in the diamond tool burnishing process. The strong polarization observed at all high angles of diffraction limits the useable efficiency in unpolarized light, but it makes such gratings very useful for tuning lasers, especially molecular lasers. The groove spacing may be chosen so that the lasing band corresponds to either the first or second of the S-plane high-efficiency plateaus. The latter will give at least twice the dispersion (in fact the maximum possible), as it is proportional to the tangent of the angle of diffraction under the Littrow conditions typical of laser tuning.

*Very-high blaze angle* gratings ( $\theta > 38^{\circ}$ ) are rarely used in the first order; their efficiency curves are interesting only because of the high P-plane values (Figure 9-10). In high orders they are often used in tuning dye lasers, where high dispersion is important and where tuning through several orders can cover a wide spectral region with good efficiency. Efficiency curves for this family of gratings are shown for two configurations. With an angular deviation of  $8^{\circ}$ , the efficiency does not differ too much from Littrow; when this angle is  $45^{\circ}$ , the deep groove results in sharp reductions in efficiency. Some of the missing energy shows up in the zeroth order, but some of it can be absorbed by the grating.

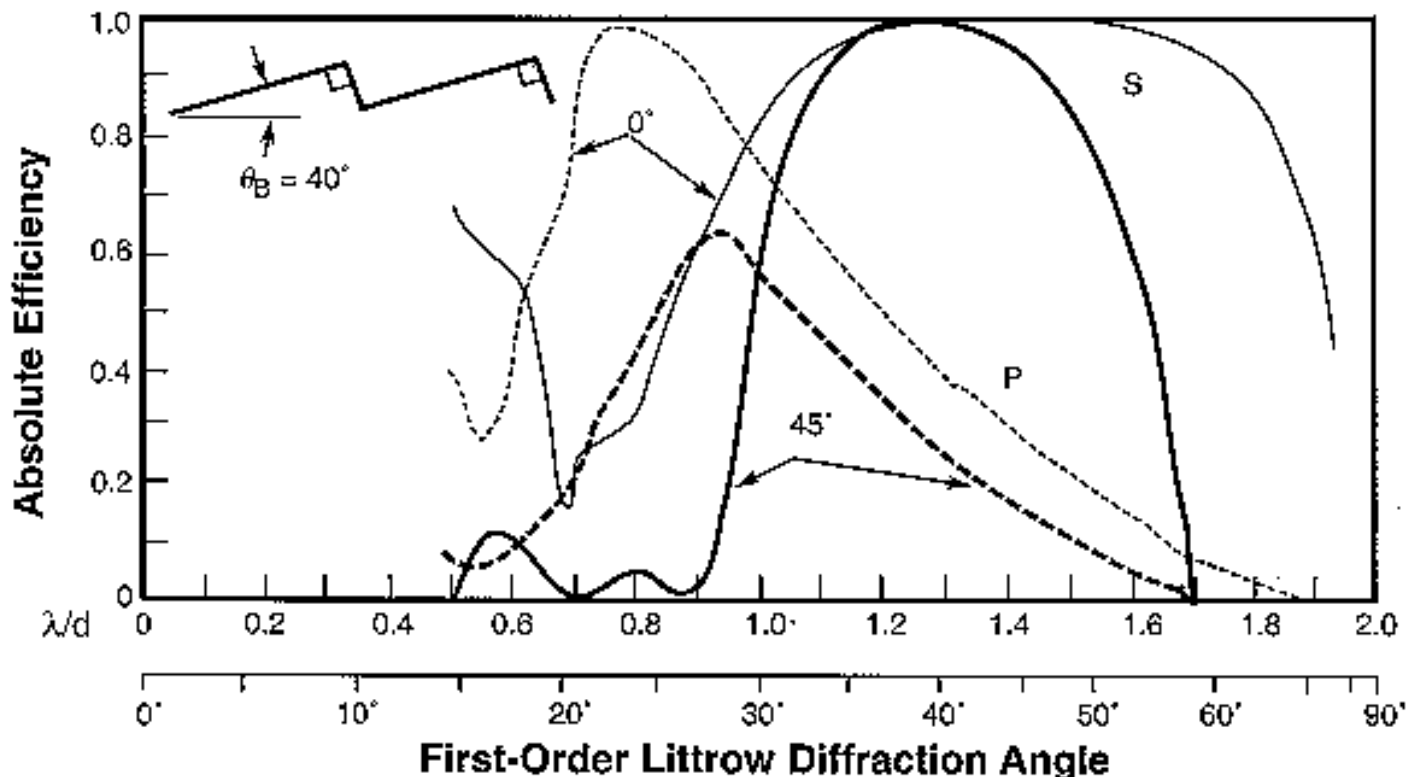


Figure 9-10. Same as Figure 9-5, except  $46^\circ$  blaze angle and  $8^\circ$  and  $45^\circ$  between the incident and diffracted beams (shown as light and heavy lines, respectively).

### 9.3. EFFICIENCY CHARACTERISTICS FOR SINUSOIDAL-GROOVE GRATINGS [\[top\]](#)

A sinusoidal-groove grating can be obtained by the interferometric (holographic) recording techniques described in [Chapter 4](#). Sinusoidal gratings have a somewhat different diffracted efficiency behavior than do triangular-groove gratings, and are treated separately.

It is convenient to consider five domains of sinusoidal-groove gratings, with progressively increasing modulation  $\mu$ , where

$$\mu = \frac{h}{d} \quad (9-1)$$

$h$  is the groove height and  $d$  is the groove spacing:[10](#)

<i>domain</i>	<i>modulation</i>
very low	$\mu < 0.05$
low	$0.05 < \mu < 0.15$
medium	$0.15 < \mu < 0.25$
high	$0.25 < \mu < 0.4$
very high	$\mu > 0.4$

*Very low modulation* gratings ( $\mu < 0.05$ ) operate in the scalar domain, where the theoretical efficiency peak for sinusoidal grooves is only 33.8% (Figure 9-11). This figure may be readily scaled, and specification is a simple matter as soon as it becomes clear that the peak wavelength always occurs at  $\lambda_B = 3.4h = 3.4\mu d$ . A blazed grating with an equivalent peak wavelength will require a groove depth 1.7 times greater.

*Low modulation* gratings ( $0.05 < \mu < 0.15$ ) are quite useful in that they have a low but rather flat efficiency over a  $\lambda/d$  band from 0.35 to 1.4 (Figure 9-12). This figure includes not only the infinite conductivity values shown on all previous ones, but includes the effects of finite conductivity by adding the curves for an 1800 g/mm aluminum surface. The most significant effect is in the behavior of the anomaly, which is the typical result of the finite conductivity of real metals.

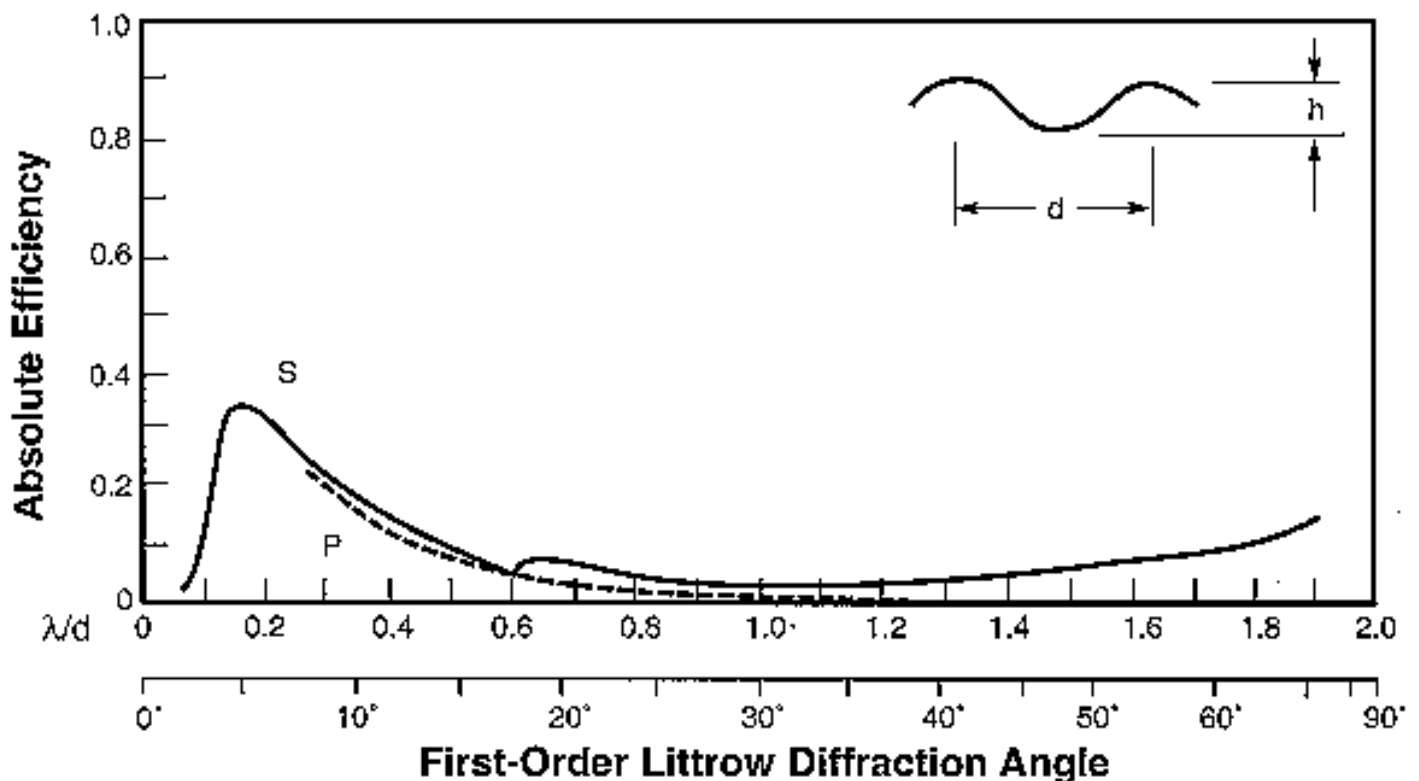


Figure 9-11. First-order theoretical efficiency curve: sinusoidal grating,  $\mu = h/d = 0.05$  and Littrow mounting ( $2K = 0$ )

Figure 9-13 is a good example of a *medium modulation* grating ( $0.15 < \mu < 0.25$ ). It demonstrates an important aspect of such sinusoidal gratings, namely that reasonable efficiency requirements confine first-order applications to values of  $\lambda/d > 0.45$ , which eliminates them from systems with wide wavelength ranges. Over this restricted region, however, efficiencies are comparable to those of triangular grooves, including the high degree of polarization. This figure also demonstrates how a departure from Littrow to an angular deviation of  $8^\circ$  splits the anomaly into two branches, corresponding to the new locations of the  $-1$  and  $+2$  order passing-off conditions.

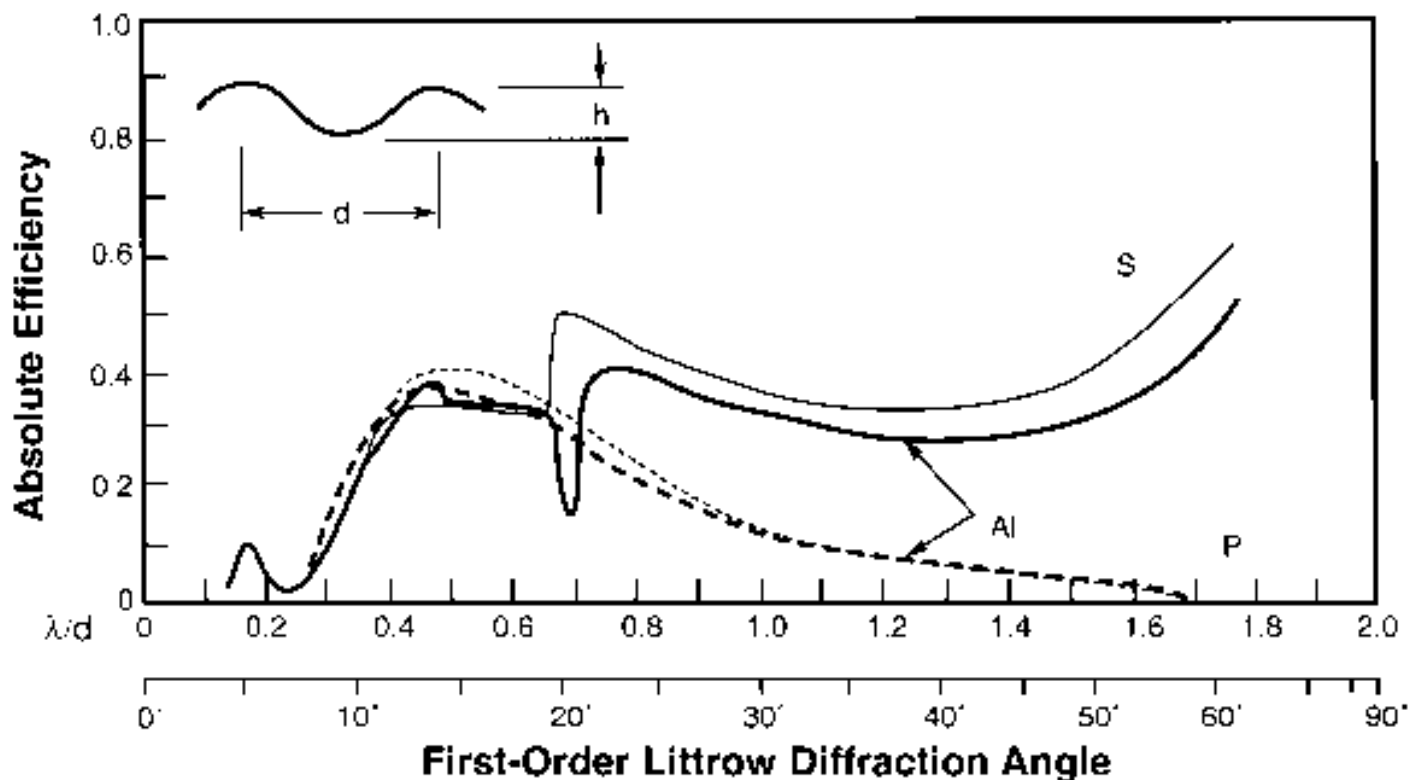


Figure 9-12. First-order theoretical efficiency curve: sinusoidal grating, aluminum coating, 1800 grooves per millimeter,  $\mu = 0.14$  and Littrow mounting. Solid curves, S-plane; dashed curves, P-plane. For reference, the curves for a perfectly conducting surface are shown as well (light curves).

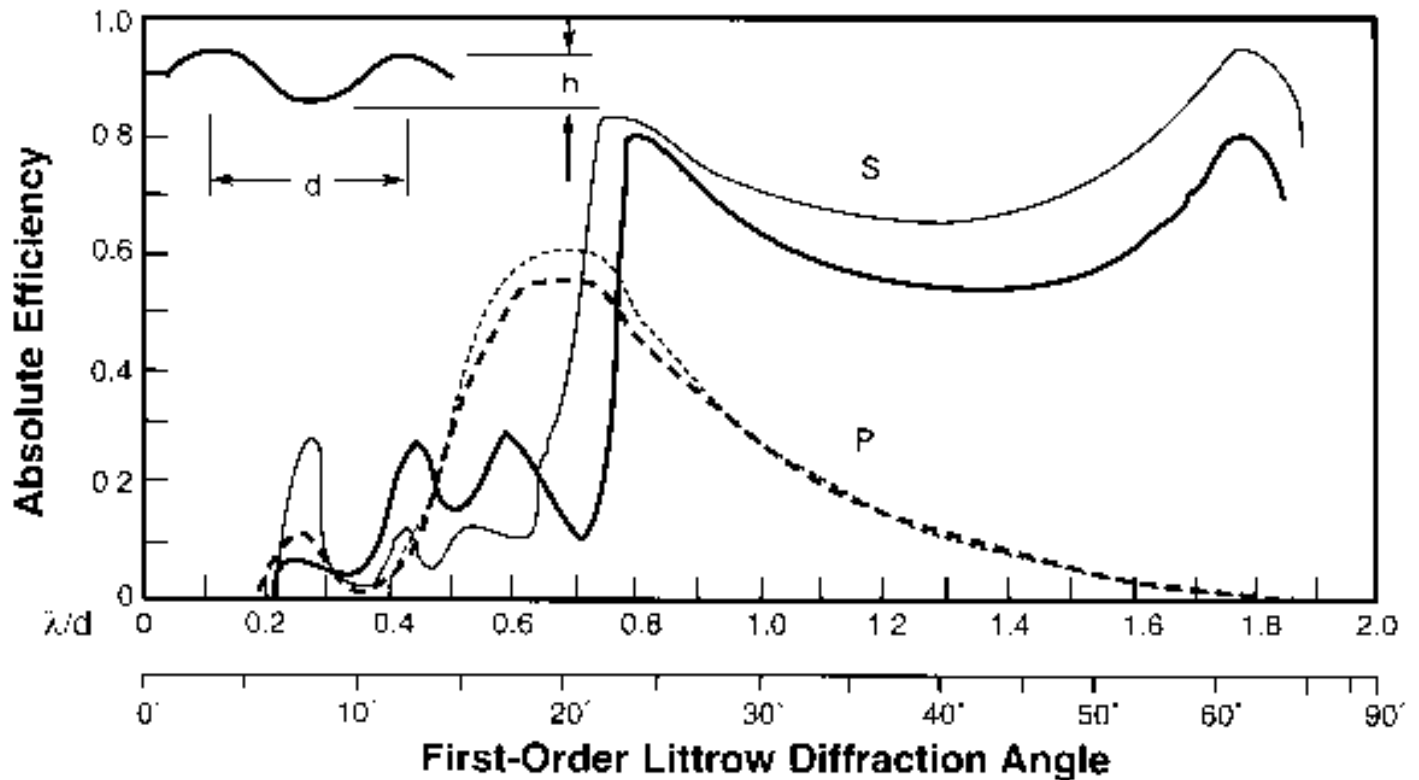


Figure 9-13. Same as Figure 9-12, except  $\mu = 0.22$  and  $8^\circ$  between incident and diffracted beams ( $2K = 8^\circ$ ).

High modulation gratings ( $0.25 < \mu < 0.40$ ), such as shown in Figure 9-14, have the maximum useful first-order efficiencies of sinusoidal-groove gratings. Provided they are restricted to the domain in which higher orders diffract (*i.e.*,  $\lambda/d > 0.65$ ), their efficiencies are very similar to those of triangular-groove gratings having similar groove depths (*i.e.*,  $26^\circ < \theta < 35^\circ$ ).

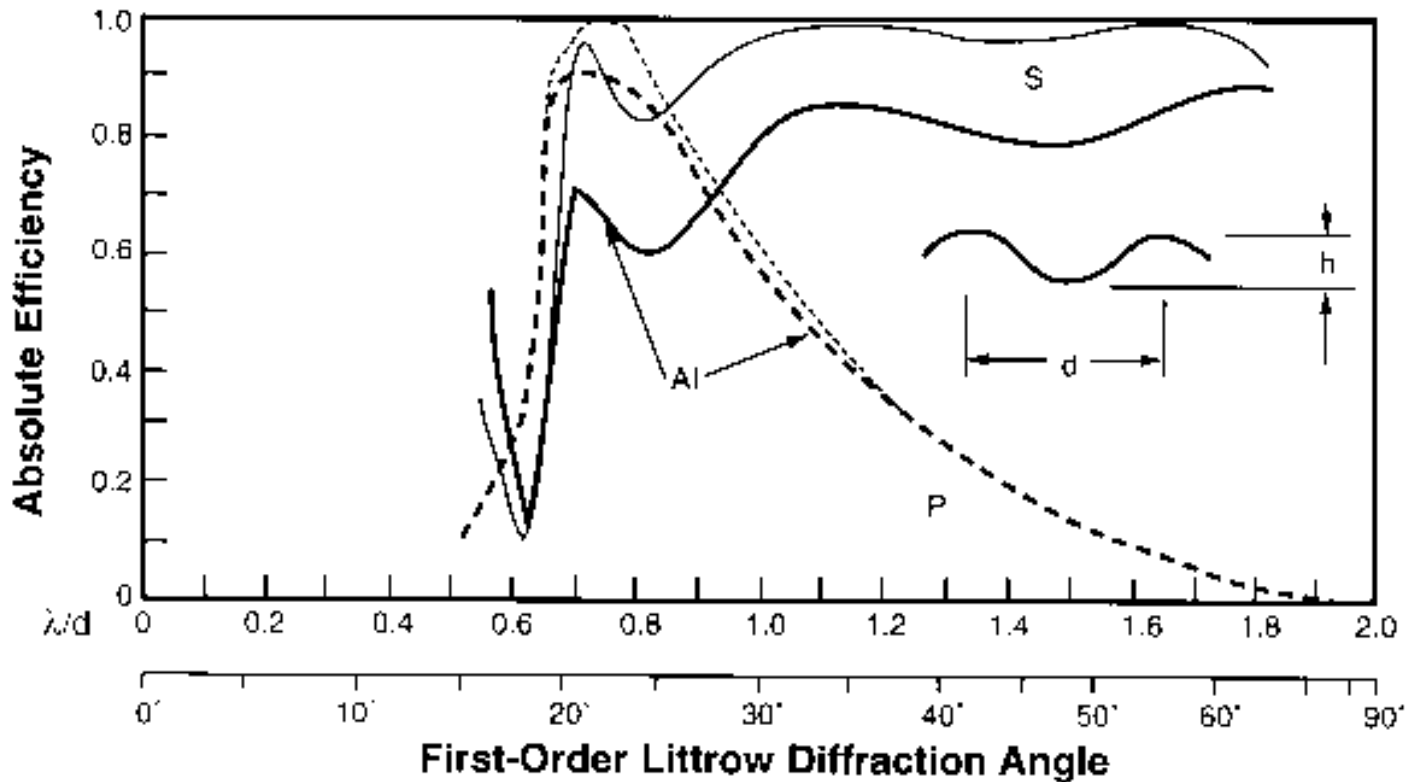


Figure 9-14. Same as Figure 9-12, except  $\mu = 0.36$ .

*Very-high modulation* gratings ( $\mu > 0.40$ ), in common with equivalent triangular-groove gratings, have little application in the first order due to their relatively low efficiencies except perhaps over narrow wavelengths ranges and for grazing incidence applications.

#### 9.4. THE EFFECTS OF FINITE CONDUCTIVITY [\[top\]](#)

For metal-coated reflection gratings, the finite conductivity of the metal is of little importance for wavelengths of diffraction above  $4 \mu\text{m}$ , but the complex nature of the dielectric constant and the index of refraction begin to effect efficiency behavior noticeably for wavelengths below  $1 \mu\text{m}$ , and progressively more so as the wavelength decreases. In the P-plane, their effect is a simple reduction in efficiency, in direct proportion to the reflectance. In the S-plane, the effect is more complicated, especially for deeper grooves and shorter wavelengths.

Figure 9-15 shows the first-order efficiency curve for a widely-used grating: 1200 g/mm, triangular grooves, medium blaze angle ( $\theta = 10^\circ$ ), coated with aluminum and used with an angular deviation of  $8^\circ$ . The finite conductivity of the metal cause a reduction in efficiency; also, severe modification of the anomaly is apparent. It is typical that the anomaly is broadened and shifted toward a longer wavelength with respect to the infinite conductivity curve. Even for an angular deviation as small as  $8^\circ$ , the single anomaly in the figure is separated into a double anomaly.

For sinusoidal gratings, the situation is shown in Figures 9-12 and 9-14. Figure 9-13 is interesting in that it clearly shows a series of new anomalies that are traceable to the role of aluminum.

With scalar domain gratings (either  $\theta < 5^\circ$  or  $\mu < 0.10$ ), the role of finite conductivity is simply to reduce the efficiency by the ratio of surface reflectance.

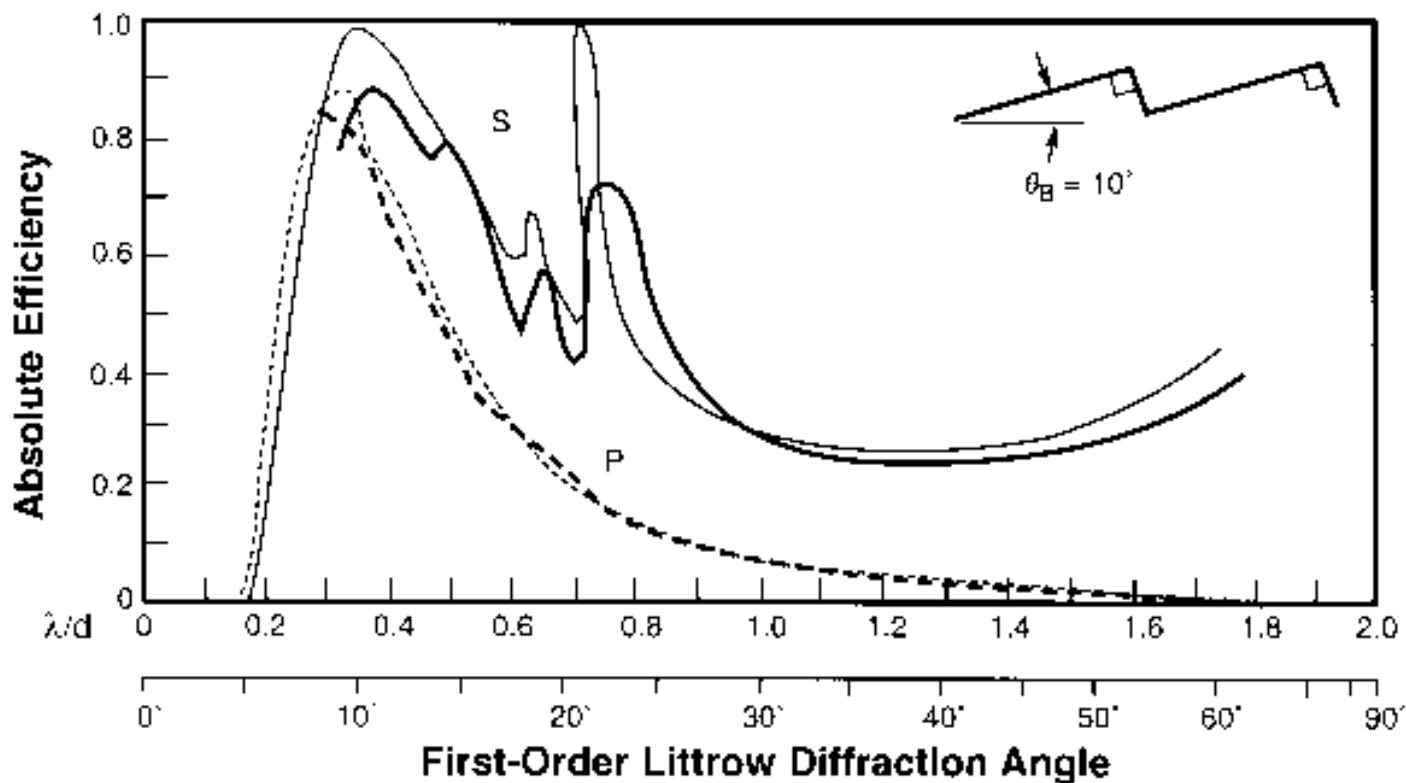


Figure 9-15. First-order theoretical efficiency curve: triangular-groove grating, aluminum coating, 1200 grooves per millimeter,  $10^\circ$  blaze angle and  $2K = 8^\circ$ . Solid curves, S-plane; dashed curves, P-plane. For reference, the curves for a perfectly conducting surface are shown as well (light curves).

## 9.5. DISTRIBUTION OF ENERGY BY DIFFRACTION ORDER [\[top\]](#)

Gratings are most often used in higher diffraction orders to extend the spectral range of a single grating to shorter wavelengths than can be covered in lower orders. For blazed gratings, the second-order peak will be at one-half the wavelength of the nominal first-order peak, the third-order peak at one-third, *etc.* Since the ratio  $\lambda/d$  will be progressively smaller as  $|m|$  increases, polarization effects will become less significant; anomalies are usually negligible in diffraction

orders for which  $|m| > 2$ . Figures 9-16 and -17 show the second- and third-order theoretical Littrow efficiencies, respectively, for a blazed grating with  $\theta = 26^\circ 45'$ ; they are plotted as a function of  $m\lambda/d$  in order to demonstrate the proper angular ranges of use. These curves should be compared with Figure 9-9 for corresponding first-order behavior.

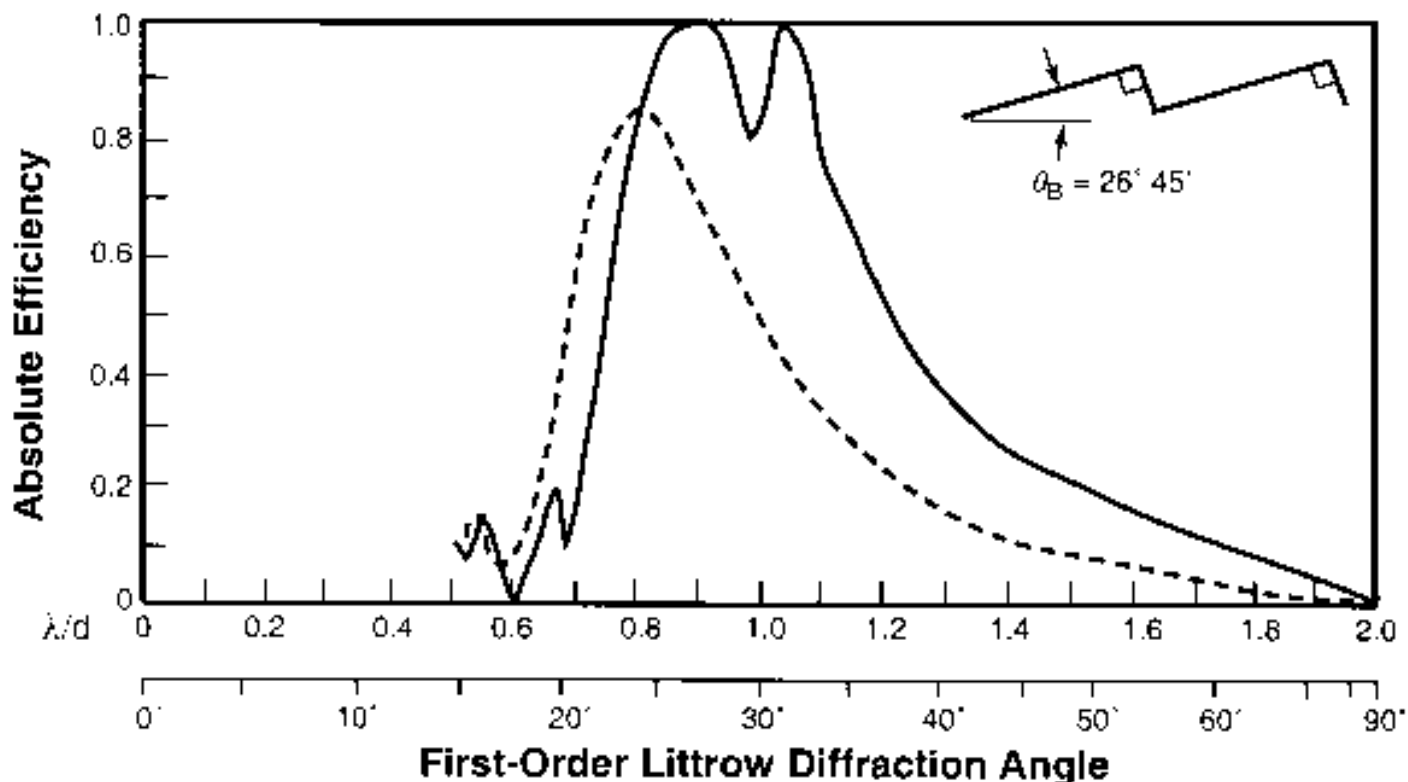


Figure 9-16. Second-order theoretical efficiency curve:  $26^\circ 45'$  blaze angle and Littrow mounting. Solid curve, S-plane; dashed curve, P-plane.

For gratings with sinusoidally shaped grooves, higher orders can also be used, but if efficiency is important, the choice is likely to be a finer pitch first-order grating instead. When groove modulations are very low (so that the grating is used in the scalar domain), the second-order efficiency curve looks similar to Figure 9-18, except that the theoretical peak value is about 23% (instead of 33.8%) and occurs at a wavelength 0.6 times that of the first-order peak, which corresponds to  $2.05h$  (instead of  $3.41h$ ), where  $h$  is the groove depth. Successive higher-order curves for gratings with sinusoidal grooves are not only closer together, but drop off more sharply with order than for gratings with triangular grooves. For sufficiently deeply modulated sinusoidal grooves, the second order can often be used effectively, though (as Figure 9-18 shows) polarization effects are relatively strong. The corresponding third-order theoretical curve is shown in Figure 9-19.



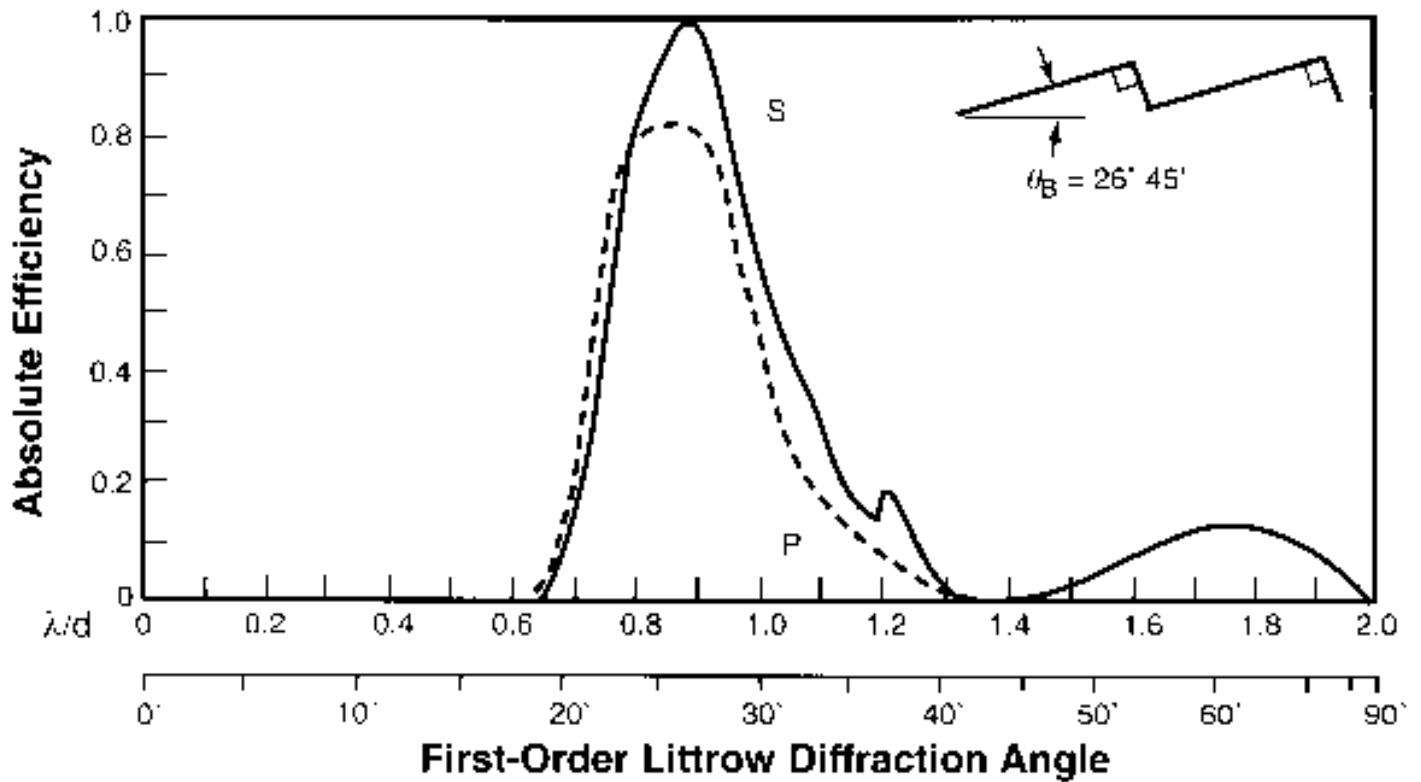


Figure 9-17. Same as Figure 9-16, except third order.

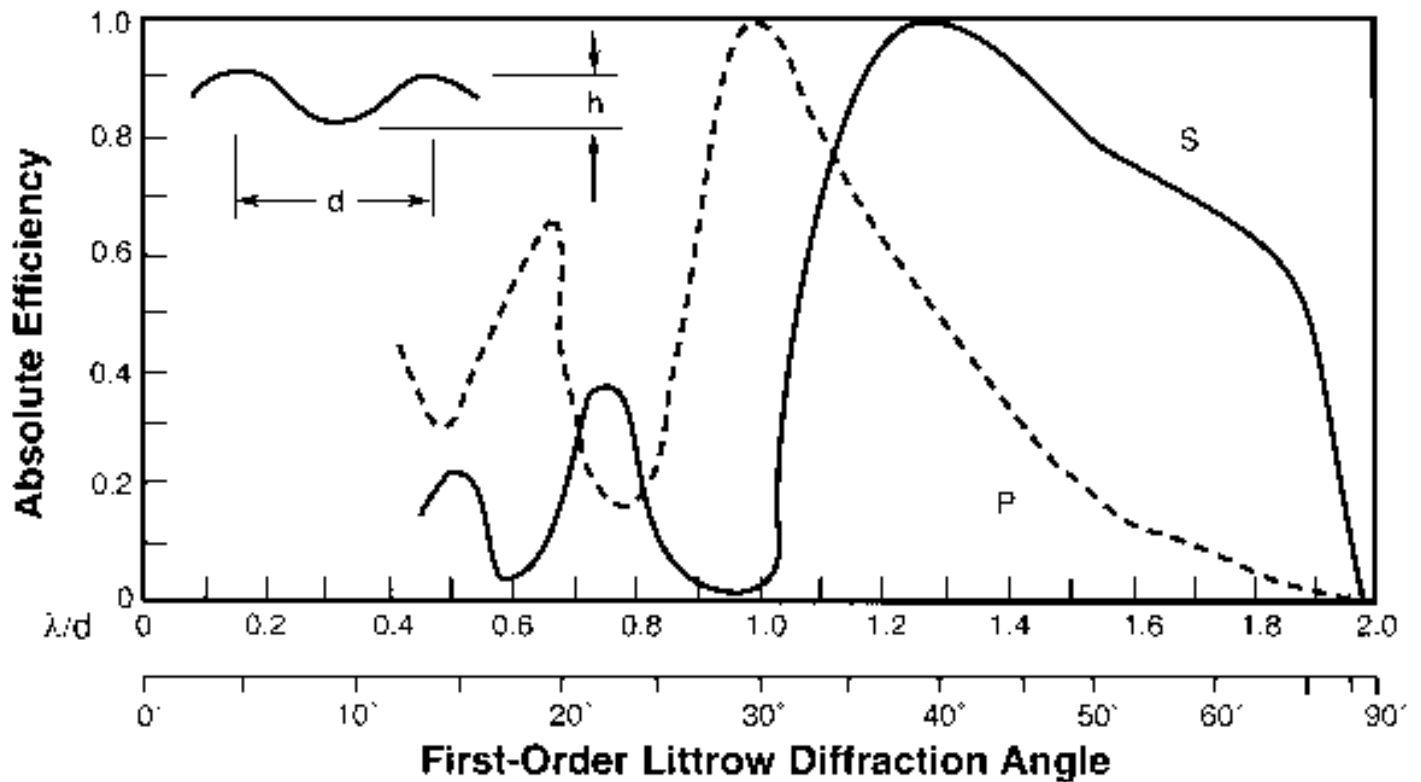


Figure 9-18. Second-order theoretical efficiency curve: sinusoidal grating,  $\mu = 0.36$  and Littrow

mounting. Solid curve, S-plane; dashed curve, P-plane.

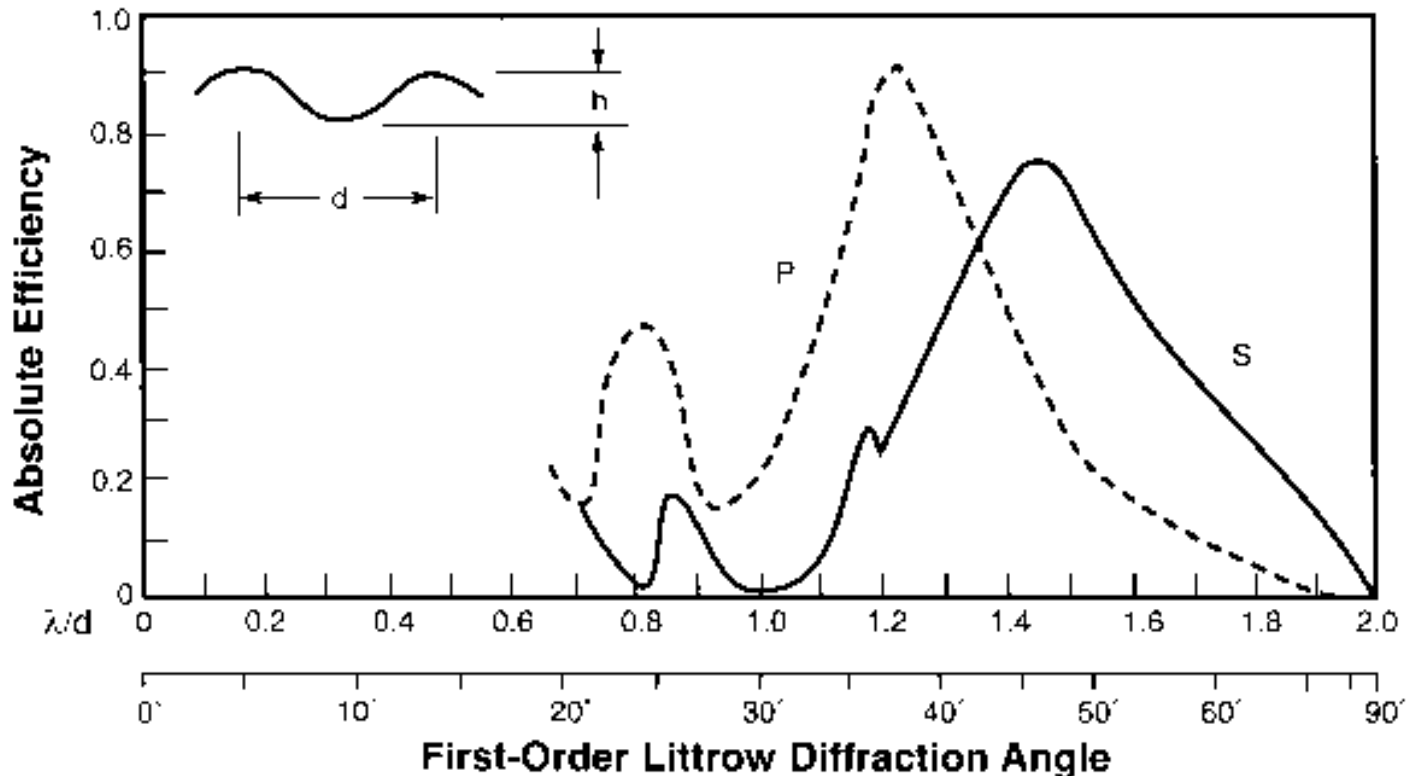


Figure 9-19. Same as Figure 9-18, except third order.

## 9.6. USEFUL WAVELENGTH RANGE [\[top\]](#)

A grating is of little use if high-grade imaging is not accompanied by sufficient diffraction efficiency. The laws governing diffracted efficiency are quite complicated, but a very rough rule of thumb can be used to estimate the useful range of wavelengths available on either side of the blaze (peak) wavelength for triangular-groove gratings.

For coarse gratings (for which  $d = 2\lambda$ ), in the first diffraction order the efficiency is roughly half its maximum (which is at  $\lambda_B$ ) at  $2\lambda_B/3$  and  $3\lambda_B/2$ . Curves of similar shape are obtained in the second and third orders, but the efficiencies are typically 20% less everywhere, as compared with the first order.

Grating of fine pitch ( $d \approx \lambda$ ) have a somewhat lower peak efficiency than do coarse gratings, though the useful wavelength range is greater.

## 9.7. BLAZING OF RULED TRANSMISSION GRATINGS [\[top\]](#)

Because they have no metallic overcoating, triangular-groove transmission gratings display far simpler efficiency characteristics than do their ruled counterparts. In particular, transmission gratings have efficiency curves almost completely free of polarization effects.

The peak wavelength generally occurs when the direction of refraction of the incident beam through a groove (thought of as a small prism) equals the direction dictated by the grating equation. [This is in direct analogy with the model of reflection grating blazing in that the grooves are thought of as small mirrors.] Due to the index of refraction of the grating, though, the groove angle exceeds the blaze angle for a transmission grating.

## 9.8. BLAZING OF HOLOGRAPHIC REFLECTION GRATINGS [\[top\]](#)

Although holographic gratings generally do not have the triangular groove profile found in ruled gratings, holographic gratings may still exhibit blazing characteristics (see, for example, Figure 9-18). For this reason it is not correct to say that all blazed gratings have triangular profiles, or that all blazed gratings are ruled gratings - blazing refers to high diffraction efficiency, regardless of the profile of the grooves or the method used to generate them.

This being said, there are some cases in which it would be preferable for a holographic grating to have a triangular groove profile rather than a sinusoidal profile. A useful technique for rendering sinusoidal groove profiles more nearly triangular is *ion etching*. By bombarding a surface with energetic ions, the material can be removed (etched) by an amount per unit time dependent on the angle between the beam and the local surface normal. The etching of a sinusoidal profile by an ion beam provides a continuously varying angle between the ion beam and the surface normal, which preferentially removes material at some parts of the profile while leaving other parts hardly etched. The surface evolves toward a triangular groove profile as the ions bombard it.

## 9.9. OVERCOATING OF REFLECTION GRATINGS [\[top\]](#)

All standard reflection gratings are furnished with an aluminum (Al) reflecting surface. While no other metal has more general application, there are a number of special situations where alternative surfaces or coatings are recommended.

The metallic coating on a reflection grating is evaporated onto the substrate. This produces a surface whose reflectivity is higher than that of the same metal electroplated onto the grating surface. The thickness of the metallic layer is chosen to enhance the diffraction efficiency

throughout the spectral region of interest.

The reflectivity of aluminum drops rather sharply for wavelengths below 170 nm. While freshly deposited, fast-fired pure aluminum in high vacuum maintains its reflectivity to wavelengths shorter than 100 nm, the thin layer of oxide normally present absorbs wavelengths below about 170 nm.

Fortunately, a method borrowed from mirror technology makes it possible to preserve the reflectivity of aluminum to shorter wavelengths. The process involves overcoating the grating with a thin layer of fast-fired aluminum, which is followed immediately by a coating of magnesium fluoride ( $\text{MgF}_2$ ) approximately 25 nm thick; the grating is kept at room temperature for both coatings. The main purpose of the  $\text{MgF}_2$  coating is to protect the aluminum from oxidation. The advantage of this coating is especially marked in the region between 120 and 170 nm. While reflectivity drops off sharply below this region, it remains higher than that of gold and comparable to that of platinum, the most commonly used alternative materials, down to 70 nm.

On an experimental basis, the use of lithium fluoride (LiF) instead of  $\text{MgF}_2$  has proved effective in maintaining relatively high reflectivity in the 100 to 110 nm region. Unfortunately, a LiF film deteriorates unless maintained in a low humidity environment, which has curtailed its use, though it can be protected by a very thin layer of  $\text{MgF}_2$ .

Gratings coated with gold (Au) and platinum (Pt) have been used for some time. Gold gratings have the great advantage that they can be replicated directly from either gold or aluminum master gratings, and are therefore most likely to maintain their groove profiles.

Overcoating gratings so that their surfaces are coated with two layers of different metals sometimes leads to a change in diffraction efficiency over time. Hunter *et al.*<sup>11</sup> have found the cause of this change to be intermetallic diffusion. For example, they measured a drastic decrease (over time) in efficiency at 122 nm for gratings coated in Au and then overcoated in Al +  $\text{MgF}_2$ ; this decrease was attributed to the formation of intermetallic compounds, primarily  $\text{AuAl}_2$  and  $\text{Au}_2\text{Al}$ . Placing a suitable dielectric layer such as SiO between the two metallic layers prevents this diffusion.

As mentioned elsewhere, fingerprints are a danger to aluminized optics. It is possible to overcoat such optics, both gratings and mirrors, with dielectrics like  $\text{MgF}_2$ , to prevent finger acids from attacking the aluminum. These  $\text{MgF}_2$  coatings cannot be baked, as is customary for glass optics, and therefore must not be cleaned with water. Spectrographic-grade organic solvents are the only recommended cleaning agents, and they should be used sparingly and with care.

Multilayer dielectric overcoatings, which are so useful in enhancing plane mirror surfaces, are of little value on a typical diffraction grating used in the visible and infrared spectra, as these coatings lead to complex guided wave effects that are rarely useful. For wavelengths below 30 nm,

though, in which grazing angles of incidence and diffraction are common, multilayer coatings can enhance efficiency considerably.<sup>[12](#)</sup>

[PREVIOUS CHAPTER](#)   [NEXT CHAPTER](#)

[Back to top](#)